HHS Public Access

Author manuscript

ACS Infect Dis. Author manuscript; available in PMC 2021 August 14.

Published in final edited form as:

ACS Infect Dis. 2020 August 14; 6(8): 2235–2248. doi:10.1021/acsinfecdis.0c00361.

Polysaccharide succinylation enhances the intracellular survival of *Mycobacterium abscessus*

Zuzana Palčeková[1], **Martine Gilleron**[2], **Shiva kumar Angala**[1], **Juan Manuel Belardinelli**[1], **Michael McNeil**[1], **Luiz E. Bermudez**[3,4], **Mary Jackson**[1,*]

[1]Mycobacteria Research Laboratories, Department of Microbiology, Immunology and Pathology, Colorado State University, Fort Collins, CO 80523-1682, USA;

[2]Institut de Pharmacologie et de Biologie Structurale, IPBS, Université de Toulouse, CNRS, UPS, 31077 Toulouse, France;

[3]Department of Biomedical Sciences, College of Veterinary Medicine, Oregon State University, Corvallis, OR 97331, USA;

[4]Department of Microbiology, College of Science, Oregon State University, Corvallis, OR 97331, USA

Abstract

Lipoarabinomannan (LAM) and its biosynthetic precursors, phosphatidylinositol mannosides (PIMs) and lipomannan (LM) play important roles in the interactions of *Mycobacterium tuberculosis* with phagocytic cells and the modulation of the host immune response but nothing is currently known of the impact of these cell envelope glycoconjugates on the physiology and pathogenicity of nontuberculous mycobacteria. We here report on the structures of *Mycobacterium abscessus* PIM, LM and LAM. Intriguingly, these structures differ from those reported previously in other mycobacterial species in several respects including the presence of a methyl substituent on one of the mannosyl residues of PIMs as well as the PIM anchor of LM and LAM, the size and branching pattern of the mannan backbone of LM and LAM, and the modification of the arabinan domain of LAM with both succinyl and acetyl substituents. Investigations into the biological significance of some of these structural oddities point to the important role of polysaccharide succinylation on the ability of *M. abscessus* to enter and survive inside human macrophages and epithelial cells and validate for the first time cell envelope polysaccharides as important modulators of the virulence of this emerging pathogen.

[*]Corresponding Author: Mary Jackson; Mary.Jackson@colostate.edu.

Authors Contributions

ZP, SKA, MG, JMB, MM, LEB and MJ designed research. ZP, MG, SKA, JMB and LEB performed research. ZP, MG, SKA, JMB, MM, LEB and MJ analyzed data. ZP, MG, SKA, JMB, MM, LEB and MJ wrote the main manuscript text. All authors reviewed the final version of the manuscript.

Supporting Information

Structural analysis of PIM and LAM, MIC determinations, comparative analysis of the ability of the wild-type and mutant strains to form biofilms *in vitro* and translocate across polarized monolayers of human A549 lung alveolar type II epithelial cells, protein sequence analysis, evidence of gene disruption at the *sucT* locus of *Mabs* ATCC 19977, colony morphology and intracellular survival of recombinant strains.

This information is available free of charge on the ACS Publications website.

The authors declare no competing financial interest.

Graphical Abstract

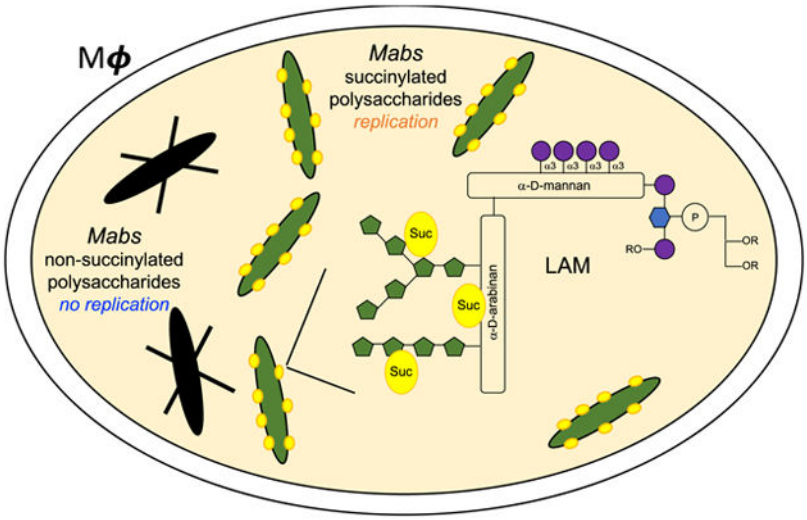

Keywords

Mycobacterium; *abscessus*; nontuberculous mycobacteria; lipoarabinomannan; arabinogalactan; succinylation

The prevalence of pulmonary nontuberculous mycobacterial (NTM) infections caused by *Mycobacterium abscessus* complex (MABSC) species including *M. abscessus* subsp. *abscessus* [*Mabs*], *M. abscessus* subsp. *massiliense* and *M. abscessus* subsp. *bolletii* is increasing worldwide, disproportionally affecting patients with structural lung disease such as chronic obstructive pulmonary disease (COPD), bronchiectasis and cystic fibrosis (CF)[1–4]. The intrinsic recalcitrance of MABSC to chemotherapeutic treatments and alarming treatment failure rates (in the range of 42 to 75%)[5] place a high priority on the development of more effective treatment approaches, a goal that may only be achieved with a better understanding of MABSC chronic infections and of the bacteria and host-related factors responsible for drug resistance and disease progression.

The distinctive cell envelope of mycobacteria is a key modulator of their interactions with the host during infection[6–7]. Yet, with the exception of surface glycopeptidolipids which have been shown to impact the biofilm-forming capacity and pathogenicity of MABSC, studies on the contribution of cell envelope constituents to NTM infections have thus far been very limited[8–14]. A group of glycolipids known as the trehalose polyphleates was recently proposed to contribute to the hyper-aggregative phenotype of rough MABSC variants[15]. A screen based on the survival of *Mabs* transposon mutants inside amoebae and macrophages has further led to the discovery of an ESX-4 type VII secretion system and of a partially characterized family of glycolipids as modulators of the intracellular survival of *Mabs*[16–17]. Despite their critical contribution to the interactions of *Mycobacterium tuberculosis* with phagocytic and non-phagocytic cells and to immunomodulation in the course of tuberculosis, the impact of lipomannan (LM), lipoarabinomannan (LAM) and

metabolic glycolipid precursors, phosphatidylinositol mannosides (PIM), in the pathogenicity of NTM has not yet been investigated[18–20]. That cell envelope (lipo)polysaccharides may contribute to NTM virulence was first suggested by Yamazaki *et al.*[21] who reported on a *Mycobacterium avium* transposon mutant impaired in biofilm formation whose virulence in mice and ability to invade bronchiolar epithelial cells were significantly reduced. Although unbeknown at the time, the transposon harbored by this mutant had disrupted a conserved gene named *sucT* which our recent work in *Mycobacterium smegmatis* established to be responsible for the succinylation of two major (lipo)polysaccharides of the mycobacterial cell envelope: arabinogalactan (AG) and LAM[22]. While the biological significance of AG and LAM succinylation remains unclear, it was recently shown that the prevalence of succinyl residues on *M. tuberculosis* LAM increased during host infection[23].

With the goal of gaining insights into the contribution of MABSC's cell envelope polysaccharides to pathogenicity, we first report on the structural characterization of PIM, LM and LAM from *Mabs* ATCC 19977 and on the unique features that distinguish these molecules from those isolated previously from other mycobacteria. Using a *sucT*-deficient mutant of the same *Mabs* isolate generated herein, we next provide the first unequivocal evidence of the involvement of cell envelope (lipo)polysaccharides in the virulence of MABSC.

RESULTS

Structural characterization of LM and LAM from *Mabs*

Overall organization of mycobacterial LM and LAM ——Since the structures of *Mabs* LM and LAM had never been previously reported, we first undertook to characterize these structures and to compare them to those of *Mtb* and other NTM. The lipid component of LM and LAM is a mannosylated phosphatidyl-*myo*-inositol moiety that serves to anchor the lipoglycans in the inner and outer membranes of the cell envelope[24] [see further in the text for a representation of LAM]. Extending from this anchor and common to LM and LAM is a linear α(1→6)-linked mannan backbone made up of 20–25 mannopyranose (Man*p*) residues elaborated by single Man*p* units which are α(1→2)-linked in the case of *M. tuberculosis* and *M. smegmatis*, but α(1→3)-linked in the case of *M. chelonae*, a *Mycobacterium* species closely related to *Mabs*[25]. In LAM, a single D-arabinan chain consisting of ~ 60 arabinofuranose (Ara*f*) residues is further attached to the mannan backbone[26]. The arabinan domain of LAM is very similar to that of AG and made of stretches of α(1→5)-linked Ara*f* residues with precisely positioned α(3→5)-branch sites. The non-reducing termini of the D-arabinan domain consist of a branched Ara_6 motif as found in AG or of a linear Ara_4[27–28]. Key to the biological activity of the entire LAM molecule is the species-specific structural micro-heterogeneity that typifies its non-reducing arabinan termini. Whereas *M. tuberculosis* and some other pathogenic slow-growing mycobacteria produce a mannoside-capped LAM (designated ManLAM), some fast-growing NTM species (e.g., *M. smegmatis* and *M. fortuitum*) instead harbor phosphoinositol caps, yielding PI-LAM, while some others are devoid of caps altogether (e.g., *M. chelonae*)[29–30]. Finally, we note the presence of succinyl residues modifying the C2 position

of a portion of the internal α−3,5-branched Ara*f* residues as well as quantitatively minor α−1,5-Ara*f* positions of the arabinan domains of AG and LAM from *M. tuberculosis*, *M. bovis* BCG and *M. smegmatis*[22,28,31–33], in addition to succinyl residues modifying the C3 position of β-(1→2)-linked Ara*f* residues of the non-reducing arabinan termini of LAM in *M. tuberculosis*[23]. Intriguingly, in *M. kansasii*, succinates were found to substitute the C3 position of linear α−1,5-Ara*f* residues rather than the internal α−3,5-branched Ara*f* residues of LAM[34].

Characterization of the mannan domain of Mabs LM and LAM ––—In order to elucidate the structure of the *Mabs* lipoglycans, we first focused on the characterization of their glycosyl composition. The glycosyl composition of LM and LAM is presented in Figure 1 and Table S1. The expected arabinose to mannose ratios were found in LAM. Surprisingly, small amounts of 2-*O*-methyl (2-*O*-Me) hexose presumed to be 2-*O*-Me mannose were seen in both LAM and LM, as well as in phosphatidylinositol dimannosides, as will be discussed further [Figure 1 A–D]. The glycosyl linkage composition of LAM and LM is shown in Table S2. We note that, like in the LAM and LM of *M. chelonae*, the dominant branched mannosyl residue is 3,6-Man*p* rather than 2,6-Man*p*. This observation was also obvious from the NMR analysis of LM and LAM. The anomeric proton region of *Mabs* LM 1D ^{1}H spectrum is dominated by two signals at 5.12 and 4.87 ppm [Figure 2B] correlating with two carbons at 105.10 and 102.15 ppm, respectively [Figure 2B]. While the former signal correlates in the TOCSY with a single H-2 at 4.06 ppm, the other correlates with two largely distinct H-2 signals at 3.97 ppm and 4.12 ppm (not shown) indicating the presence of two anomeric protons at 4.87 ppm. The three spin systems were assigned to *t*-Man*p* (IV), 6-Man*p* (VI) and 3,6-Man*p* (VIII) [Table 1] in accordance with published literature[25,33,35–37]. The same three spin systems (IV, VI, VIII) were also observed in the ^{1}H-^{13}C HMQC of LAM [Figure 2A]. No 2,6-Man*p* could be observed by NMR despite small amounts being detected by glycosyl linkage analysis [Table S2] suggesting that the 2,6-Man*p* identified with the latter method was in fact undermethylated 6-Man*p*.

The mass spectrum of deacylated *Mabs* LM [Figure 3A] showed that its size was considerably bigger than that of *M. smegmatis* LM which averages 23–29 residues[38] in that *Mabs* LM averaged 32–44 mannosyl residues. LM with an even number of mannosyl residues also predominated although significant amounts of LM with an odd number of mannosyl residues was also present. Intriguingly, after digestion with α−1,6-endomannanase from *Bacillus circulans* TN-31[38], large mannans (free from the reducing mannosylated phosphatidyl-*myo*-inositol moiety) were produced and they were all of even masses [Figure 3B]. The large mannans were approximately six mannosyl residues shorter than the intact *Mabs* LM suggesting a region of non-branched α−1,6-linked mannosyl residues next to the inositol as in the mannan from *M. smegmatis* LM[38]. A Man_4 tetrasaccharide was also released in large amounts upon endomannanase digestion [Figure 3C]. It cannot be a linear α−1,6-linked mannosyl tetrasaccharide or it would have been further degraded by the enzyme. It must thus reflect the mannan branching pattern but both its structure and its location on the mannan backbone remain to be elucidated.

Characterization of the lipid anchor of Mabs LM and LAM ——GC/MS analysis of fatty acid methyl esters prepared from WT *Mabs* LM and LAM revealed the presence of C14:0 and C15:0 besides the fatty acids typically found esterifying the lipid anchor of *M. tuberculosis* or *M. smegmatis* LM and LAM (C16:0, C18:0, C18:1, tuberculostearic acid) [Table S3]. Thus, similar to *M. chelonae*, the lipid anchor of *Mabs* LM and LAM is acylated with a greater variety of fatty acids than typically seen in *M. tuberculosis*[39]. Unlike the situation in *M. chelonae*[25], however, the relative distribution of fatty acids differed between LM and LAM. Whereas C16:0 was the most abundant fatty acid found in both lipoglycans (representing 36.2 and 66% of the total fatty acid content of WT LM and LAM, respectively), comparable amounts of C18:0 (32.9%) was found in LM whereas in LAM, C18:0 only represented ~9% of the total fatty acids. Conversely, more C14:0 was found esterifying the lipid anchor of WT LAM than WT LM (14% vs 0.9%).

We next sought to elucidate the origin of the 2-*O*-Me hexose residues identified in LM and LAM [Figure 1 A–B and D]. Since this residue was also found on purified phosphatidylinositol dimannosides [Figure 1C], we believed that the methyl group is located on a Man*p* residue of the phosphatidylinositol anchor. In support of this hypothesis, LC/MS analysis of deacylated *Mabs* LM indicated that each LM species was 14 mass units higher than predicted from its component parts [Figure 3A] suggesting that all molecules of the LM contained the 2-*O*-Me mannosyl residue. To map its location, deacylated *Mabs* LM was next digested with α−1,6-endomannanase. The digestion released phosphatidyl-*myo*-inositol dimannoside (also known as PIM_2) with *m/z* 671.1805 $[M\text{-}H]^-$ instead of *m/z* 657.1541 $[M\text{-}H]^-$ confirming that the methylation of *Mabs* LM occurs on its reducing end [Figure 3B]. Since PIM_2 also exist as free glycolipids populating in abundance mycobacterial membranes in the form of monoacylated PIM_2 (Ac_1PIM_2) and diacylated PIM_2 (Ac_2PIM_2), we used PIM_2 for further analyses of the location of the methyl group. PIM_2 were purified from the total lipid extracts from WT *Mabs* and deacylated. In agreement with our analysis of alditol acetates derived from deacylated PIM_2 [Figure 1C], LC/MS analysis of the purified deacylated material revealed a compound with *m/z* 671.1805 $[M\text{-}H]^-$ consistent with the methylation of PIM_2 [Figure S1]. Thus, one of the two mannosyl residues on PIM_2 was methylated. To determine which one, purified acylated PIM_2 were next submitted to NMR analysis. The methyl group was clearly observed on the 1D ^1H spectrum of Ac_2PIM_2 in D_2O as a singlet at 3.23 ppm and identified by the correlation between this proton and a carbon at 58.56 ppm on the ^1H-^{13}C HMQC spectrum [Figure 4]. COSY (not shown) and ^1H-^{13}C HMQC [Figure 4] data allowed for the assignment of the different spin systems [Table 2], in agreement with previous studies[35]. Significant differences between the H2 chemical shifts of both mannose units pointed to the presence of a methyl group on Man1 as its C2 is shifted downfield (79.78 ppm) compared with the Man2 C2 (69.73 ppm). This is supported by the observation on the ROESY spectrum of a noe contact between the methyl group and the Man1 H1 (4.97 ppm) and a correlation between the methyl group and the Man1 C2 (79.78 ppm) on the ^1H-^{13}C HMBC spectrum [Figure S2].

Characterization of the arabinan domain of Mabs LAM ——Glycosyl linkage analysis showed that the arabinan portion of LAM possesses the typical linkages found in other mycobacterial LAMs [Table S2] with a number of branches (based on 2-Ara*f*:5-Ara*f*

molar ratio) very similar to that reported for *M. smegmatis* LAM[22]. Similarly, ^{1}H-^{13}C HMQC spectrum [Figure 2A] and ^{1}H-^{1}H TOCSY [Figure 5] highlighted the classical footprints of the different arabinose spin systems previously described[33]: 5-*O*-Ara*f* (I), 3,5-α-Ara*f* (II), 2-Ara*f* (III) and *t*-Ara*f* (V). LC/MS analysis of the oligoarabinosides released upon *Cellulomonas gelida* endoarabinanase digestion of *Mabs* LAM revealed an equal proportion of linear Ara_4 and branched Ara_6 arabinan termini [Table S4]. In contrast to *M. smegmatis* and *M. tuberculosis* LAM which harbor phosphoinositol or mannoside caps, respectively, at their non-reducing arabinan termini, further analysis of the *Mabs* digestion products indicated an absence of capping motifs as was reported in *M. chelonae*[25] [Figure S3]. This analysis also indicated that the oligoarabinosides released by WT *Mabs* LAM after digestion with *Cellulomonas gelida* endoarabinanase may be modified by a succinyl group and/or an acetyl group with the individual modified oligosaccharides representing 14.5% (succinylated Ara_4), 7.6% (acetylated Ara_4), 0.9% (both modifications) of the total pool of Ara_4, and 5.8% (succinylated Ara_6) and 7.3% (acetylated Ara_6) of the total pool of Ara_6 [Table S4]. Low amounts of succinylated Ara_2 (8.9%) were also detected.

Wild-type LAM was further analyzed for the presence of these succinylated and acetylated residues by 1D and 2D NMR spectroscopy[22,25,33]. The 1D ^{1}H spectrum showed the characteristic two pseudo-triplets of similar intensities at 2.48 and 2.63 ppm [Figure 6A and B] assigned to methylene groups of succinyl units. Their corresponding carbons were characterized at 34.7 and 33.3 ppm, respectively, on the 2D ^{1}H-^{13}C HMQC spectrum [Figure 6B]. Besides these residues, two singlets at 2.13 and 2.04 ppm correlating with two carbons at 23.2 and 25.2 ppm, respectively, define two acetyl groups. All these protons (at 2.48, 2.63, 2.13 and 2.04 ppm) showed a correlation with carbons around 180 ppm typifying carbonyl groups (not shown). The cross-peak between ^{1}H 4.92/^{13}C 82.1 further typifies the presence of succinyl residues on the C2 of −3,5-Ara*f* residues, as described by Delmas *et al.*[33].

In light of the results of our structural analyses, the MABSC LAM structure represented on Figure 7 is proposed.

Disruption of *sucT* in *Mabs* –: Given the proposed involvement of the succinyl substituents of *M. tuberculosis* LAM in pathogenicity[23], we next sought to generate a succinyl-deficient mutant of *Mabs*. A search for orthologs of the SucT succinyltransferase of *M. tuberculosis* (Rv1565c) and *M. smegmatis* (MSMEG_3187) identified one candidate in *Mabs* ATCC 19977. MAB_2689 shares 61% identity (73 % similarity) and 58% identity (69 % similarity) with its *M. tuberculosis* and *M. smegmatis* counterparts (with a 100% coverage), respectively, and displays the expected secondary structure and conserved cytoplasmic and transmembrane functional amino acid residues of prokaryotic trans-acylases (COG1835) involved in the *O*-acylation of carbohydrates[40–42] [Figure S4].

MAB_2689 (*sucT*) was disrupted by homologous recombination, yielding *Mabs*Δ*sucT* [Figure S5]. A complemented mutant strain was generated by expressing in *Mabs*Δ*sucT* a wild-type (WT) copy of the *Mabs sucT* gene from the integrative plasmid pMV306-*sucT.* Preliminary analysis of the lipoglycans from the WT, mutant and complemented mutant strains by SDS-PAGE showed that the migration profile of the mutant LAM was altered

[Figure 8], as expected of a form LAM having undergone a change in charge as a result of losing succinyl residues[22]. The migration profile of the mutant LAM reverted back to WT upon complementation with *sucT* expressed from pMV306, but not when the empty pMV306 plasmid was used [Figure 8].

***Mabs*Δ*sucT* produces lipoglycans structurally similar to those of WT *Mabs* except for the loss of succinyl groups on LAM –:** The impact of disrupting *sucT* on the succinylation of LAM was first verified by GC/MS upon butanolysis of LAM prepared from the WT, mutant and complemented mutant strains to yield dibutyl esters of any succinyl groups present[22]. This analysis revealed an almost complete absence of succinates in the mutant LAM which were essentially restored in the complemented mutant. Quantitation of succinyl to arabinosyl residues showed a ratio of 1:327 (S.D., ±20 for two determinations) for the mutant strain, 1:20 (S.D., ± 4 for four determinations) for the WT strain, and 1:22.5 (S.D., ± 1.5 for three determinations) for *Mabs*Δ*sucT*/pMV306-*sucT* [Figure 9]. The absence of succinates on the mutant LAM was further confirmed by comparative LC/MS analysis of the oligoarabinosides released by the WT, mutant and complemented mutant LAM upon digestion with *Cellulomonas gelida* endoarabinanase. Whereas oligoarabinosides bearing acetyl substituents were detected in the LAM digestion products from all three strains, succinylated oligoarabinosides were missing from the *Mabs*Δ*sucT* LAM [Table S4]. Finally, the 1D ^{1}H and 2D ^{1}H-^{13}C HMQC spectra of the mutant LAM [Figure 6C] confirmed the absence of signals typifying the succinyl groups and their restoration upon genetic complementation [Figure 6D], whereas the signals and correlations revealing the acetyl groups remained present in the mutant LAM [Figure 6C].

Quantitative analyses of the alditol acetate and per-*O*-methylated alditol acetate derivatives of the WT, mutant and complemented mutant LAM otherwise did not point to any significant alterations in the Ara*f* to Man*p* ratio of the mutant LAM [Table S1] or increase in the degree of branching of its mannan and arabinan domains [Table S2]. The relative proportion of Ara_4 to Ara_6 arabinan termini of LAM was also similar in the WT and mutant strains [Table S4] as was the fatty acyl composition of their LM and LAM lipid anchors [Table S3].

***Mabs*Δ*sucT* produces an AG devoid of succinyl residues on the arabinan domain –:** Given the involvement of SucT from *M. smegmatis* in the succinylation of both LAM and AG[22], we next probed the degree of succinylation of AG in the WT, mutant and complemented mutant strains by subjecting their purified mycolyl-AG-peptidoglycan (mAGP) complex to the same butanolysis procedure as for LAM. The mutant mAGP showed a dramatic decrease in succinate content relative to WT mAGP which was restored to WT levels in the complemented mutant strain [Figure 9]. Quantitation of succinyl to arabinosyl residues yielded a ratio of 1:59 (S.D., ± 12 for two determinations) for the WT strain, 1:382 (S.D., ± 4 for two determinations) for *Mabs*Δ*sucT*, and 1:80 (S.D., ± 24 for two determinations) for *Mabs*Δ*sucT*/pMV306-*sucT.* The fact that *Mabs*Δ*sucT* mAGP was not entirely devoid of succinates as per the butanolysis analysis could indicate that succinyl groups substitute, in a SucT-independent manner, some other positions of AG or of the peptidoglycan or mycolic acid moieties of mAGP.

Analyses of the monosaccharide composition [Table S5] and glycosyl linkages [Table S6] of the WT, mutant and complemented mutant AG otherwise failed to reveal any significant structural alterations in the galactan or arabinan domains of the mutant AG. The degree of mycolylation of the mutant AG was also similar to that measured in the WT and complemented mutant strains [Table S5].

Alterations in the cell surface properties of the *Mabs sucT* mutant –: Because *sucT* mutants of *M. marinum*, *M. avium* and *M. smegmatis* had previously been reported to differ from their WT parent in terms of their cell surface properties reflecting in colony morphology, surface hydrophobicity, biofilm-forming capacity and/or propensity to aggregate in liquid broth[22,43–44], we first set out to compare the phenotypes of the *Mabs* WT, mutant and complemented mutant in a panel of *in vitro* assays.

Monitoring of the absorbance of *Mabs* cultures over time in 7H9-ADC-tyloxapol medium at 37°C pointed to a slight reduction in growth of the *sucT* knockout in that the mutant never quite reached the same high cell density as the WT and complemented mutant strains did [Figure 10A]. This phenotype was not due to the hyper-aggregation of the mutant cells. Comparable to the situation with the *M. smegmatis sucT* knockout mutant[22], we found *Mabs*Δ*sucT* to bind ~ 3 times more Congo Red than the WT and complemented strains, pointing to an increase in its cell surface hydrophobicity [Figure 10B]. Differences in Congo red binding also reflected on TS agar supplemented with Congo Red where the WT and complemented mutant strains grew as white colonies whereas *Mabs*Δ*sucT* grew as red colonies [Figure 10B]. Since Congo red is known to bind polysaccharides, we verified that this difference in Congo red binding was not due to the differential binding of the dye to succinylated versus non-succinylated LAM in the cells. The results, which are presented in Figure S6, show that Congo Red actually does not bind any variant of the lipoglycan, despite showing evidence of binding to the positive control, carboxymethylcellulose.

Other phenotypic tests essentially yielded negative results. Unlike *M. smegmatis* and *M. avium sucT* knock-outs[22,43], *Mabs*Δ*sucT* displayed a WT colonial morphology on 7H11-OADC agar [Figure S7A]. To our surprise, and in striking contrast with the situation in *M. avium*[43], *Mabs*Δ*sucT* was also as proficient at forming biofilms as its WT parent [Figure S7B]. Under the culture conditions tested therein, the *Mabs* knock-out also did not display the hyper-aggregative phenotype characteristic of *M. smegmatis* and *M. marinum sucT* mutants[22,44]. Finally, comparison of the sliding motility of the WT and mutant strains on 7H9-ADC agar with or without 0.05% Tween-80 did not reveal any obvious differences between strains (data not shown).

Drug susceptibility testing using different classes of antibiotics used in the clinical treatment of NTM infections did not point to any noticeable alterations in the susceptibility of the *sucT* mutant to antibiotics [Table S7]. Finally, because of the negative charge imparted by succinate and acetate on LAM and AG and of the known impact of the charge of LPS and teichoic acids on the susceptibility of Gram-negative and Gram-positive bacteria to cationic antimicrobial peptides[45–48], we compared *Mabs*Δ*sucT* to its WT parent for their level of resistance to LL-37 and HNP-1. The MICs of both peptides against the *Mabs* strains tested

herein were very high (>100 μg mL^{-1}), however, no dramatic increase in the susceptibility of the *sucT* mutant was noted [Table S7].

Impaired replication and intracellular survival of the *Mabs sucT* mutant in macrophages and epithelial cells –: Since changes in the cell surface hydrophobicity of *Mabs* caused by a deficiency in LAM and/or AG succinylation might have impacted the way the bacterium interacted with host cells, we next proceeded to compare the uptake and intracellular survival of the *Mabs* WT, *sucT* knock-out and complemented mutant strain in human monocyte-derived THP-1 macrophages, A549 lung alveolar type II epithelial cells and BEAS-2B bronchial mucosal epithelial cells. A significant reduction in entry of the mutant compared to the WT and complemented mutant were noted in THP-1 macrophages and A549 epithelial cells [Figure 11A–B]. In all cellular models tested, the mutant further showed reduced intracellular survival compared to the WT parent [Figure 11A–C]. Survival in all cell types was restored to WT levels in the complemented mutant. A comparison of the ability of the three *Mabs* strains to translocate across polarized monolayers of human A549 lung alveolar type II epithelial cells, in contrast, failed to reveal any impact of the loss of AG and LAM succinylation [Table S8].

Inhibition of reactive oxygen species by treatment with superoxide dismutase and of phagosome acidification by treatment with bafilomycin A1 both significantly enhanced the ability of *Mabs* WT and complemented mutant strains to replicate inside THP-1 macrophages [Figure S8]. In contrast, the same treatments had a much more modest effect on the intracellular replication and persistence of *Mabs*Δ*sucT* indicating that a combination of factors most likely accounts for the reduced ability of the knock-out mutant to survive inside macrophages.

DISCUSSION

The studies described therein reveal for the first time the structures of *Mabs* PIM, LM and LAM [Figure 7] and support polysaccharides as key cell envelope constituents modulating the virulence of MABSC.

In common with the closely related species, *M. chelonae*, *Mabs* LAM is devoid of capping motifs at the non-reducing arabinan termini, and the mannan domain of both LM and LAM harbors α−1,3-Man*p* side chains instead of the α−1,2-Man*p* side chains normally found in *M. smegmatis* and *M. tuberculosis*. The size of the mannan domain of *Mabs* LM (33–44 mannosyl residues) is considerably larger than that of *M. smegmatis* (23–29 mannosyl residues). As has been reported in *M. tuberculosis*, *M. smegmatis* and a number of other tuberculous and nontuberculous mycobacteria[22–23,28,33–34,49], succinyl substituents modify the LAM and AG of *Mabs*. While their position on AG was not precisely determined in this study, we were able to map these modifications to the C2 of α−3,5-Ara*f* residues and other as yet incompletely defined positions of the arabinan termini of LAM. We further identified the succinyltransferase encoded by *MAB_2689* (*sucT*) as the sole enzyme responsible for their addition onto the lipoglycan. Most strikingly and unique among all mycobacterial LMs and LAMs whose structures have been reported to date, is the presence of acetyl substituents

modifying the arabinan termini of LAM and the finding of a methylated mannopyranosyl residue linked to position 6 of the *myo*-inositol residue of PIM, LM and LAM.

In *M. tuberculosis*, the transfer of a Man*p* to position 6 of the *myo*-inositol residue of PIM is mediated by the GDP-Man*p*-dependent mannosyltransferase PimB'[50]. In line with the methylation of this Man*p* residue in *Mabs* but not in any other mycobacteria analyzed to date, we note that *Mabs pimB'* (*MAB_1976*) maps in the genome of *Mabs* ATCC19977 right upstream a gene annotated as a putative *S*-adenosyl-methionine-dependent methyltransferase (*MAB_1977*). Only nine base-pairs separate the stop codon of *pimB'* from the start codon of *MAB_1977* indicating that the two genes may be co-transcribed. Orthologs of *MAB_1977* were found in the genomes of a few NTM species including *M. immunogenum*, *M. chelonae* and *M. talmoniae*, as well as in some *Nocardia*, but were noticeably absent from *M. tuberculosis*, *M. avium*, *M. smegmatis* and *M. leprae*.

The modification of LPS with discrete covalent substituents such as acyl chains, phosphates, aminosugars, phosphoethanolamine and methyl groups is a well-established strategy used by Gram-negative bacteria to promote adaptation and survival under various stress conditions. For instance, another pathogen of the CF lung, *Pseudomonas aeruginosa*, has been reported to modify the lipid A and O-antigen moieties of LPS with acyl groups, aminosugars and methyl substituents to modulate acute versus chronic infection and evade detection by the host[47,51]. Much less is known of the biological significance of the discrete covalent substituents found on mycobacterial LAM[52] despite indications that succinyl residues may become more prevalent on *M. tuberculosis* LAM during host infection[23]. To gain insight into the biological significance of succinyl substituents, a *sucT* knock-out mutant of *Mabs* ATCC 19977 was constructed and submitted to a panel of biochemical analyses and phenotypic assays *in vitro* and *ex vivo*. In line with previous observations made on a *M. smegmatis sucT* mutant[22], succinylation of AG and LAM in *Mabs* had no apparent impact on the biosynthesis of these polysaccharides, or on the mycolylation of AG. These findings contrast with the report of a *M. marinum sucT* mutant in which various aspects of LAM biosynthesis were found to be impaired, including mannoside capping, acylation of the phosphatidylinositol mannoside anchor and branching of the mannan and arabinan domains[23]. Based on these observations, it thus seems unlikely that succinyl substituents act as conserved molecular signals governing the biosynthesis of AG and LAM in slow and fast-growing mycobacteria. A common trait of all mycobacterial *sucT* mutants generated to date, however, relates to their altered surface properties reflecting in one or more of the following phenotypes: Changes in colony morphology (*M. avium* and *M. smegmatis*)[22,43], reduced biofilm forming capacity (*M. avium*)[44], hyper-aggregation (*M. smegmatis* and *M. marinum*)[22,44], and increased surface hydrophobicity (*M. smegmatis, Mabs*) and rigidity (*M. smegmatis*)[22]. It is thus reasonable to propose that the succinylation of the two major cell envelope polysaccharides of mycobacteria serves to modulate - most likely through indirect, charge-mediated, effects - the cell surface properties of the bacilli. Because the composition of the cell envelope varies across *Mycobacterium* species, as does the structure of LAM that bears some of these substituents, it is to be expected that the qualitative and quantitative impact of succinylation will be species-dependent. The different effects associated with AG and LAM succinylation on the interactions of *Mabs* and *M. avium* with host cells further supports this assumption. Whereas a *M. avium sucT* mutant was significantly impaired in its

ability to invade BEAS-2B human bronchiolar epithelial cells[21] while displaying no apparent uptake or replication phenotype in THP-1 macrophages[53], the corresponding *Mabs* mutant was not as dramatically impaired in BEAS-2B invasion but displayed reduced uptake by both THP-1 macrophages and A549 epithelial cells, and much reduced intracellular survival in all cell types analyzed in this study. Clearly, while conserved in slow- and fast-growing, pathogenic and non-pathogenic, *Mycobacterium* species, the biological significance of polysaccharide succinylation in mycobacteria is contextual and more studies will be required to decipher their physiological and pathogenic impact as well as the underlying molecular mechanisms. Apparently more restricted in distribution across mycobacteria are the acetyl and methyl substituents of PIM, LM and LAM. The acetates bring additional negative charges to those conferred by the succinates to specific regions of the arabinan domain of LAM and may play a similar role in modulating the interactions of MABSC with host cells. The methylation of PIM and of the lipid anchor of LM and LAM, on the other hand, somewhat increases the hydrophobicity of these molecules and may impact the integrity and the permeability of the inner and outer membranes in which they are anchored.

METHODS

Bacterial strains and growth conditions –

Mabs ATCC 19977 was grown under agitation at 37°C in Middlebrook 7H9 medium supplemented with 10% albumin-dextrose-catalase (ADC) (BD Sciences) and 0.05% Tween 80, in cation-adjusted Mueller Hinton II broth (BD Sciences) with 0.05% tyloxapol, in Tryptic Soy (TS) broth with 0.05% tyloxapol, or on Middlebrook 7H11 agar supplemented with 10% oleic acid-albumin-dextrose-catalase (OADC) (BD Sciences). Zeocin (Zeo) and kanamycin (Kan) were added to the culture media at a final concentration of 100 μg ml^{-1}.

Mabs sucT knock-out mutant –

Recombineering was used to inactivate the *sucT* (*MAB_2689*) gene of *Mabs* ATCC 19977 by allelic replacement. To this end, the Gp60 and Gp61 recombineering proteins from mycobacteriophage Che9c were expressed from the replicative plasmid pJV53-XylE under control of an acetamide-inducible promoter[54–55]. Acetamide-induced *Mabs* ATCC 19977 harboring pJV53-XylE were electro-transformed with ~ 500 ng of linear allelic exchange substrate consisting of the Zeo resistance cassette bracketed by ~500-bp of upstream and downstream homologous DNA sequence flanking *sucT*. Double crossover candidates were selected on Zeo-containing plates and confirmed by PCR. For complementation, the entire coding sequence of *Mabs sucT* was PCR-amplified from *Mabs* ATCC 19977 genomic DNA and cloned into the integrative plasmid pMV306, yielding pMV306-*sucT.* Primer sequences for all constructs are available upon request.

Preparation of lipids, lipoglycans and arabinogalactan –

Extraction of total lipids, lipoglycans and the mycolyl-AG-peptidoglycan (mAGP) complex from *Mabs* cells followed procedures described earlier for the characterization of the *M. smegmatis sucT* mutant[22]. Lipoglycans were purified by gel exclusion chromatography[56] and analyzed by SDS-PAGE on commercial Novex™ 10–20% Tricine gels stained with

periodic acid Schiff reagent. Polar lipids from WT *Mabs* ATCC 19977 were precipitated from the total lipid extract with acetone at 4°C overnight, and PIM_2 were further purified from the precipitate by chromatography on a silicic acid column (1.5 × 20 cm) (KG60, 230–400 mesh, Supelco) as described previously[57]. Purified PIM_2 were dried and deacylated using a 33% methylamine solution in ethanol:water:water saturated butanol (69:23:8) at room temperature overnight (modified protocol from ref.[58].

Analytical procedures –

Structural analyses of PIMs, lipoglycans and mAGP followed earlier procedures[22]. Briefly, 1 mg of mAGP, 20 μg of acylated PIM_2 and 50 μg of LAM were used for permethylation and alditol acetates preparation and analyzed by GC/MS to determine monosaccharide composition and glycosyl linkage patterns. Digestion of LM with endo-α-(1→6)-D-mannanase from *Bacillus circulans* and analysis of the products of the reaction by LC/MS followed the procedure recently described by Angala *et al.*[38]. Succinates were analyzed and quantified by GC/MS analysis as their butyl succinate derivatives obtained from either 20 μg of purified LAM or 1 mg of mAGP. The presence of potential capping motifs at the non-reducing arabinan termini of LAM from *Mabs* was analyzed by LC/MS after digestion of LAM with *Cellulomonas gelida* endoarabinanase. Deacylated PIM_2 and the endoarabinanase digestion products of LAM were directly analyzed by ultra-performance liquid chromatography (UPLC) on an Atlantis T3 column (Waters) using Waters Acquity UPLC H-Class system coupled to a Bruker MaXis Plus QTOF MS instrument according to the method described by De *et al.*[23].

The fatty acids esterifying the mannosylated phosphatidyl-*myo*-inositol anchor of LM and LAM were analyzed as their fatty acid methyl esters (FAME) by GC/MS. Briefly, 100 μg of LM and LAM were methanolyzed in 100 μl of 3M methanolic HCl by heating at 80°C overnight and extracted with *n*-hexane:water (1:1). FAMEs were analyzed on a Thermo Scientific TRACE 1310 Gas Chromatograph paired with a Thermo Scientific TSQ 8000 Evo Triple Quadrupole GC-MS/MS. Samples were run on a 30 m × 0.25 mm × 0.25 μm Zebron ZB-5HT Inferno capillary column (Phenomenex) at an initial temperature of 60°C. The temperature was increased to 375°C at a ramp rate of 20°C min^{-1} and held for 5 min. Data handling was carried out using the Thermo Scientific Chromeleon Chromatography Data System software.

Mycolic acids released from mAGP by treatment with 2 M trifluoroacetic acid were quantified by LC/MS as described earlier[59] on an Agilent 1260 Infinity chromatograph equipped with a 2.1 mm × 150 mm (3.5 μm particle size) XBridge reverse phase C18 column (Waters) coupled to an Agilent 6224 time-of-flight (TOF) mass spectrometer. Data were analyzed using the Agilent MassHunter software.

NMR experiments were performed at 298K with a cryo-probed Bruker DRX600 spectrometer (Karlsruhe, Germany) and a Prodigy™ cryo-probed Bruker Avance-IV 400 MHz NEO spectrometer for the 2D ^{1}H-^{13}P HMQC sequences. Native molecules were dissolved in D_2O (LM and LAM) or $CDCl_3/CD_3OD/D_2O$ 60/35/8 (PIM) and analyzed in 200 × 5 mm 535-PP NMR tubes. Proton and carbon chemical shifts are expressed in ppm

downfield from the signal of external acetone (δH 2.22 and δC 30.89) and those of Ac_2PIM_2 are expressed in ppm downfield from the signal of chloroform (δH 7.26 and δC 77.36).

Congo Red binding and sliding motility –

M. smegmatis strains were tested for Congo red binding in TS broth and TS agar as described by Etienne *et al.*[60]. For testing the ability of LAM to bind Congo red, 5 μg of LAM from *Mabs* WT and *Mabs*Δ*sucT*, and 5 μg of carboxymethylcellulose (low viscosity, Sigma) were dot-blotted on a nitrocellulose membrane and either stained with Congo red (1 mg ml^{-1} Congo red solution in 0.1 mol L^{-1} acetate buffer (pH 3.3)) or immunodetected with CS-35 antibodies. Congo red staining was performed for 45 min at room temperature with subsequent destaining in water for 30 min at room temperature. For sliding motility assays, *Mabs* strains were drop-inoculated from liquid cultures diluted to 10^6 CFU mL^{-1} onto 7H9-ADC medium containing 0.34% agar with or without 0.05% Tween 80 and incubated at 37°C for 5 days.

Biofilm assay –

Static biofilms were formed in Hanks' balanced salt solution (HBSS) or 7H9-OADC as previously described[61] with minor modifications. Briefly, bacteria were taken from 7H10-OADC agar plates and resuspended in either HBSS or 7H9-OADC to generate a bacterial suspension of ~ 10^7 CFU mL^{-1}. 150 μL of this suspension was seeded in 96-well polystyrene (BD, Franklin Lakes, NJ) and the biofilms allowed to establish for 10 days in the dark at 25°C. Biofilm biomass was determined by plating and counting CFUs.

Drug susceptibility testing –

MIC values were determined in cation-adjusted Mueller-Hinton II broth in a total volume of 100 μl in 96-well microtiter plates. *Mabs* cultures grown to early log phase were diluted to a final concentration of 10^6 CFU mL^{-1} and incubated in the presence of serial dilutions of the drugs for 4 days at 37°C. MICs were determined using the resazurin blue test[62].

Macrophage infection and survival assays –

Human monocyte THP-1 cells (ATCC) were cultured in suspension in RPMI-1640 (Corning) supplemented with 10% fetal bovine serum (FBS, Gemini) at 37°C with 5% CO_2. Cells were counted with a hemocytometer, seeded at 80% confluency into 24-well plates and supplemented with 20 ng mL^{-1} phorbol 12-myristate 13-acetate (PMA, Sigma Aldrich) to trigger differentiation into adherent macrophages. After 24 hours, the culture medium was replaced and cells were allowed to rest for an additional 24 hours prior to infection. THP-1 cells were infected with well-dispersed suspensions of the WT, mutant and complemented mutant strains in PBS at a multiplicity of infection of 10 bacteria per cell for one hour at 37°C in a 5% CO_2 atmosphere. Infected cells were then gently washed twice with HBSS and added fresh culture medium supplemented with 100 μg mL^{-1} amikacin (Sigma) for 2 hours to kill extracellular bacteria. In some experiments, the culture medium was supplemented with 50 μg mL^{-1} superoxide dismutase or 13 nM bafilomycin A1 to inhibit reactive oxygen species and vacuolar acidification, respectively. Upon two washes with HBSS, the wells were lysed 2 hours, 2 days and 4 days post-infection with 0.1% Triton X-100 for 10 to 15

minutes and the cell lysates were serially diluted in PBS and plated onto Middlebrook 7H10-OADC agar to count CFUs. Colonies were counted after 5 days of incubation at 37°C. A modified Trypan blue test was used to monitor the integrity of the monolayer throughout the infection.

Infection of lung epithelial cells –

A549 lung alveolar type II epithelial cell line (ATCC) was cultured in DMEM (Corning) supplemented with 10% FBS at 37°C with 5% CO_2. Human BEAS-2B bronchial mucosal epithelial cells (CRL-9609) were cultured as described in ref.[21] in BEBM medium supplemented with BEGM which contains bovine pituitary extract (BPE), hydrocortisone, human epidermal growth factor (hEGF), epinephrine, transferrin, insulin, retinoic acid, and triiodothyronine (Lonza, Allendale, NJ). Cell infections with *Mabs* were as described for the THP-1 cells except that the infection was synchronized by centrifugation for 5 min at 232 × *g* after addition of the bacteria. Killing of extracellular bacteria, cell lysis and CFU counting were as described for THP-1 cells.

Polarized cell layer translocation assay –

A549 epithelial cells grown in DMEM supplemented with 5% FBS were seeded at 2×10^5 cells per well on the 6.5 mm porous filter membrane of a transwell insert (Corning, Tewksbury, MA). Polarized monolayer achieved confluence after 5 days at 37°C in a 5% CO_2 atmosphere. Trans-epithelial resistance was measured using a Millicell-ESR apparatus (Millipore) as per the manufacturer's instructions, right at the beginning and at the end of the infection. Final values were obtained by subtracting the blank value, and the results are expressed as ohms/cm^2. A modified Trypan blue test was also used to monitor the integrity of the monolayer. To determine bacterial translocation through the monolayer, dispersed bacteria were placed in the upper chamber (at a MOI of 10) and the supernatant of the basal chamber was plated after 24 hours of infection on 7H10-OADC agar for CFU enumeration.

Supplementary Material

Refer to Web version on PubMed Central for supplementary material.

ACKNOWLEDGMENTS

This work was supported by the National Institute of Allergy and Infectious Diseases/National Institutes of Health grant AI064798 (to MJ), and an award from the Cystic Fibrosis Foundation (to MJ). The content is solely the responsibility of the authors and does not necessarily represent the official views of the NIH or the Cystic Fibrosis Foundation. We thank the Integrated Screening Platform of Toulouse (PICT, IBiSA) for providing access to 600 MHz equipment, Dr. John Spencer (Colorado State University) for the provision of CS-35 antibodies, and Dr. Delphi Chatterjee and Anita Amin (Colorado State University) for the provision of *Cellulomonas gelida* endoarabinanase.

REFERENCES

1. Prevots DR, and Marras TK (2015) Epidemiology of human pulmonary infection with nontuberculous mycobacteria: a review. Clin Chest Med 36, 13–34 [PubMed: 25676516]
2. Park IK, and Olivier KN (2015) Nontuberculous mycobacteria in cystic fibrosis and non-cystic fibrosis bronchiectasis. Semin Respir Crit Care Med 36, 217–224 [PubMed: 25826589]

3. Martiniano SL, Nick JA, and Daley CL (2019) Nontuberculous Mycobacterial Infections in Cystic Fibrosis. Thorac Surg Clin 29, 95–108 [PubMed: 30454926]
4. Bryant JM, Grogono DM, Rodriguez-Rincon D, Everall I, Brown KP, Moreno P, Verma D, Hill E, Drijkoningen J, Gilligan P, Esther CR, Noone PG, Giddings O, Bell SC, Thomson R, Wainwright CE, Coulter C, Pandey S, Wood ME, Stockwell RE, Ramsay KA, Sherrard LJ, Kidd TJ, Jabbour N, Johnson GR, Knibbs LD, Morawska L, Sly PD, Jones A, Bilton D, Laurenson I, Ruddy M, Bourke S, Bowler IC, Chapman SJ, Clayton A, Cullen M, Dempsey O, Denton M, Desai M, Drew RJ, Edenborough F, Evans J, Folb J, Daniels T, Humphrey H, Isalska B, Jensen-Fangel S, Jonsson B, Jones AM, Katzenstein TL, Lillebaek T, MacGregor G, Mayell S, Millar M, Modha D, Nash EF, O'Brien C, O'Brien D, Ohri C, Pao CS, Peckham D, Perrin F, Perry A, Pressler T, Prtak L, Qvist T, Robb A, Rodgers H, Schaffer K, Shafi N, van Ingen J, Walshaw M, Watson D, West N, Whitehouse J, Haworth CS, Harris SR, Ordway D, Parkhill J, and Floto RA (2016) Emergence and spread of a human-transmissible multidrug-resistant nontuberculous mycobacterium. Science 354, 751–757 [PubMed: 27846606]
5. Wu ML, Aziz DB, Dartois V, and Dick T (2018) NTM drug discovery: status, gaps and the way forward. Drug Discov Today 23, 1502–1519 [PubMed: 29635026]
6. Daffé M, and Draper P (1998) The envelope layers of mycobacteria with reference to their pathogenicity. Adv Microb Physiol 39, 131–203 [PubMed: 9328647]
7. Jackson M (2014) The Mycobacterial Cell Envelope-Lipids. Cold Spring Harbor perspectives in medicine 4, a021105 DOI: 10.1101/cshperspect.a021105 [PubMed: 25104772]
8. Howard ST, Rhoades E, Recht J, Pang X, Alsup A, Kolter R, Lyons CR, and Byrd TF (2006) Spontaneous reversion of *Mycobacterium abscessus* from a smooth to a rough morphotype is associated with reduced expression of glycopeptidolipid and reacquisition of an invasive phenotype. Microbiology 152, 1581–1590 [PubMed: 16735722]
9. Nessar R, Reyrat JM, Davidson LB, and Byrd TF (2011) Deletion of the mmpL4b gene in the Mycobacterium abscessus glycopeptidolipid biosynthetic pathway results in loss of surface colonization capability, but enhanced ability to replicate in human macrophages and stimulate their innate immune response. Microbiology 157, 1187–1195 [PubMed: 21292749]
10. Jonsson B, Ridell M, and Wold AE (2013) Phagocytosis and cytokine response to rough and smooth colony variants of Mycobacterium abscessus by human peripheral blood mononuclear cells. APMIS 121, 45–55 [PubMed: 23030647]
11. Bernut A, Herrmann JL, Kissa K, Dubremetz JF, Gaillard JL, Lutfalla G, and Kremer L (2014) Mycobacterium abscessus cording prevents phagocytosis and promotes abscess formation. Proc Natl Acad Sci U S A 111, E943–952 [PubMed: 24567393]
12. Roux AL, Viljoen A, Bah A, Simeone R, Bernut A, Laencina L, Deramaudt T, Rottman M, Gaillard JL, Majlessi L, Brosch R, Girard-Misguich F, Vergne I, de Chastellier C, Kremer L, and Herrmann JL (2016) The distinct fate of smooth and rough Mycobacterium abscessus variants inside macrophages. Open Biol 6 DOI: 10.1098/rsob.160185
13. Whang J, Back YW, Lee KI, Fujiwara N, Paik S, Choi CH, Park JK, and Kim HJ (2017) Mycobacterium abscessus glycopeptidolipids inhibit macrophage apoptosis and bacterial spreading by targeting mitochondrial cyclophilin D. Cell Death Dis 8, e3012 DOI: 10.1038/cddis.2017.420 [PubMed: 28837151]
14. Malcolm KC, Caceres SM, Pohl K, Poch KR, Bernut A, Kremer L, Bratton DL, Herrmann JL, and Nick JA (2018) Neutrophil killing of Mycobacterium abscessus by intra- and extracellular mechanisms. PLoS One 13, e0196120 DOI: 10.1371/journal.pone.0196120 [PubMed: 29672589]
15. Llorens-Fons M, Perez-Trujillo M, Julian E, Brambilla C, Alcaide F, Byrd TF, and Luquin M (2017) Trehalose Polyphleates, External Cell Wall Lipids in Mycobacterium abscessus, Are Associated with the Formation of Clumps with Cording Morphology, Which Have Been Associated with Virulence. Front Microbiol 8, 1402 DOI: 10.3389/fmicb.2017.01402 [PubMed: 28790995]
16. Laencina L, Dubois V, Le Moigne V, Viljoen A, Majlessi L, Pritchard J, Bernut A, Piel L, Roux AL, Gaillard JL, Lombard B, Loew D, Rubin EJ, Brosch R, Kremer L, Herrmann JL, and Girard-Misguich F (2018) Identification of genes required for Mycobacterium abscessus growth in vivo with a prominent role of the ESX-4 locus. Proc Natl Acad Sci U S A 115, E1002–E1011 [PubMed: 29343644]

17. Dubois V, Viljoen A, Laencina L, Le Moigne V, Bernut A, Dubar F, Blaise M, Gaillard JL, Guerardel Y, Kremer L, Herrmann JL, and Girard-Misguich F (2018) MmpL8MAB controls Mycobacterium abscessus virulence and production of a previously unknown glycolipid family. Proc Natl Acad Sci U S A 115, E10147–E10156 [PubMed: 30301802]

18. Mishra AK, Driessen NN, Appelmelk BJ, and Besra GS (2011) Lipoarabinomannan and related glycoconjugates: structure, biogenesis and role in Mycobacterium tuberculosis physiology and host-pathogen interaction. FEMS Microbiol Rev 35, 1126–1157 [PubMed: 21521247]

19. Vergne I, Gilleron M, and Nigou J (2014) Manipulation of the endocytic pathway and phagocyte functions by Mycobacterium tuberculosis lipoarabinomannan. Front Cell Infect Microbiol 4, 187 DOI: 10.3389/fcimb.2014.00187 [PubMed: 25629008]

20. Turner J, and Torrelles JB (2018) Mannose-capped lipoarabinomannan in Mycobacterium tuberculosis pathogenesis. Pathog Dis 76 DOI: 10.1093/femspd/fty026

21. Yamazaki Y, Danelishvili L, Wu M, Hidaka E, Katsuyama T, Stang B, Petrofsky M, Bildfell R, and Bermudez LE (2006) The ability to form biofilm influences Mycobacterium avium invasion and translocation of bronchial epithelial cells. Cell Microbiol 8, 806–814 [PubMed: 16611229]

22. Palcekova Z, Angala SK, Belardinelli JM, Eskandarian HA, Joe M, Brunton R, Rithner C, Jones V, Nigou J, Lowary TL, Gilleron M, McNeil M, and Jackson M (2019) Disruption of the SucT acyltransferase in *Mycobacterium smegmatis* abrogates succinylation of cell envelope polysaccharides. J Biol Chem 294, 10325–10335 [PubMed: 31110045]

23. De P, Shi L, Boot C, Ordway D, McNeil M, and Chatterjee D (2020) Comparative Structural Study of Terminal Ends of Lipoarabinomannan from Mice Infected Lung Tissues and Urine of a Tuberculosis Positive Patient. ACS Infect Dis 6, 291–301 [PubMed: 31762254]

24. Pitarque S, Larrouy-Maumus G, Payré B, Jackson M, Puzo G, and Nigou J (2008) The immunomodulatory lipoglycans, lipoarabinomannan and lipomannan, are exposed at the mycobacterial cell surface. Tuberculosis 88, 560–565 [PubMed: 18539533]

25. Guérardel Y, Maes E, Elass E, Leroy Y, Timmerman P, Besra GS, Locht C, Strecker G, and Kremer L (2002) Structural study of lipomannan and lipoarabinomannan from *Mycobacterium chelonae*. J. Biol. Chem 277, 30635–30648 [PubMed: 12063260]

26. Kaur D, Angala SK, Wu SW, Khoo KH, Chatterjee D, Brennan PJ, Jackson M, and McNeil MR (2014) A single arabinan chain is attached to the phosphatidylinositol mannosyl core of the major immunomodulatory mycobacterial cell envelope glycoconjugate, lipoarabinomannan. J. Biol Chem 289, 30249–30256 [PubMed: 25231986]

27. Shi L, Berg S, Lee A, Spencer JS, Zhang J, Vissa V, McNeil MR, Khoo K-H, and Chatterjee C (2006) The carboxy terminus of EmbC from *Mycobacterium smegmatis* mediates chain length extension of the arabinan in lipoarabinomannan. J. Biol. Chem 281, 19512–19526 [PubMed: 16687411]

28. Bhamidi S, Scherman MS, Rithner CD, Prenni JE, Chatterjee D, Khoo K-H, and McNeil MR (2008) The identification and location of succinyl residues and the characterization of the interior arabinan region allows for a model of the complete primary structure of *Mycobacterium tuberculosis* mycolyl arabinogalactan. J. Biol. Chem 283, 12992–13000 [PubMed: 18303028]

29. Gilleron M, Jackson M, Nigou J, and Puzo G (2008) Structure, activities and biosynthesis of the Phosphatidyl-*myo*-Inositol-based lipoglycans in The Mycobacterial Cell Envelope (Daffé M, and Reyrat J-M eds.), ASM Press, Washington, DC pp 75–105

30. Angala SK, Belardinelli JM, Huc-Claustre E, Wheat WH, and Jackson M (2014) The cell envelope glycoconjugates of Mycobacterium tuberculosis. Crit Rev Biochem Mol Biol 49, 361–399 [PubMed: 24915502]

31. Weber PL, and Gray GR (1979) Structural and immunochemical characterization of the acidic arabinomannan of Mycobacterium smegmatis. Carbohydr Res 74, 259–278 [PubMed: 573662]

32. Hunter SW, Gaylord H, and Brennan PJ (1986) Structure and antigenicity of the phosphorylated lipopolysaccharide antigens from the leprosy and tubercle bacilli. J. Biol. Chem 261, 12345–12351 [PubMed: 3091602]

33. Delmas C, Gilleron M, Brando T, Vercellone A, Gheorghiu M, Rivière M, and Puzo G (1997) Comparative structural study of the mannosylated-lipoarabinomannans from *Mycobacterium bovis*

BCG vaccine strains: characterization and localization of succinates. Glycobiology 7, 811–817 [PubMed: 9376683]

34. Guérardel Y, Maes E, Briken V, Chirat F, Leroy Y, Locht C, Strecker G, and Kremer L (2003) Lipomannan and lipoarabinomannan from a clinical isolate of *Mycobacterium kansasii:* Novel structural features and apoptosis-inducing properties. J. Biol. Chem 278, 36637–36651 [PubMed: 12829695]
35. Gilleron M, Nigou J, Cahuzac B, and Puzo G (1999) Structural study of the lipomannans from *Mycobacterium bovis* BCG: characterisation of multiacylated forms of the phosphatidyl-*myo*-inositol anchor. J Mol Biol 285, 2147–2160 [PubMed: 9925791]
36. Gilleron M, Bala L, Brando T, Vercellone A, and Puzo G (2000) *Mycobacterium tuberculosis* H37Rv parietal and cellular lipoarabinomannans. Characterization of the acyl- and glyco-forms. J. Biol. Chem 275, 677–684 [PubMed: 10617666]
37. Nigou J, Gilleron M, Brando T, Vercellone A, and Puzo G (1999) Structural definition of arabinomannans from Mycobacterium bovis BCG. Glycoconj J 16, 257–264 [PubMed: 10579694]
38. Angala SK, Li W, Palcekova Z, Zou L, Lowary TL, McNeil MR, and Jackson M (2019) Cloning and Partial Characterization of an Endo-alpha-(1->6)-d-Mannanase Gene from Bacillus circulans. Int J Mol Sci 20 DOI: 10.3390/ijms20246244
39. Nigou J, Gilleron M, and Puzo G (2003) Lipoarabinomannans: From structure to biosynthesis. Biochimie 85, 153–166 [PubMed: 12765785]
40. Slauch JM, Lee AA, Mahan MJ, and Mekalanos JJ (1996) Molecular characterization of the oafA locus responsible for acetylation of Salmonella typhimurium O-antigen: oafA is a member of a family of integral membrane trans-acylases. J Bacteriol 178, 5904–5909 [PubMed: 8830685]
41. Thanweer F, Tahiliani V, Korres H, and Verma NK (2008) Topology and identification of critical residues of the O-acetyltransferase of serotype-converting bacteriophage, SF6, of Shigella flexneri. Biochem Biophys Res Commun 375, 581–585 [PubMed: 18755141]
42. Thanweer F, and Verma NK (2012) Identification of critical residues of the serotype modifying O-acetyltransferase of Shigella flexneri. BMC biochemistry 13, 13 DOI: 10.1186/1471-2091-13-13 [PubMed: 22793174]
43. Yamazaki Y, Danelishvili L, Wu M, Macnab M, and Bermudez LE (2006) Mycobacterium avium genes associated with the ability to form a biofilm. Appl Environ Microbiol 72, 819–825 [PubMed: 16391123]
44. Driessen NN, Stoop EJ, Ummels R, Gurcha SS, Mishra AK, Larrouy-Maumus G, Nigou J, Gilleron M, Puzo G, Maaskant JJ, Sparrius M, Besra GS, Bitter W, Vandenbroucke-Grauls CM, and Appelmelk BJ (2010) Mycobacterium marinum MMAR_2380, a predicted transmembrane acyltransferase, is essential for the presence of the mannose cap on lipoarabinomannan. Microbiology 156, 3492–3502 [PubMed: 20688818]
45. Raetz CRH, Reynolds CM, Trent MS, and Bishop RE (2007) Lipid A modification systems in Gram-negative bacteria. Annu. Rev. Biochem 76, 295–329 [PubMed: 17362200]
46. Swoboda JG, Campbell J, Meredith TC, and Walker S (2010) Wall teichoic acid function, biosynthesis, and inhibition. Chembiochem 11, 35–45 [PubMed: 19899094]
47. Needham BD, and Trent MS (2013) Fortifying the barrier: the impact of lipid A remodelling on bacterial pathogenesis. Nat Rev Microbiol 11, 467–481 [PubMed: 23748343]
48. Schneewind O, and Missiakas D (2014) Lipoteichoic acids, phosphate-containing polymers in the envelope of gram-positive bacteria. J Bacteriol 196, 1133–1142 [PubMed: 24415723]
49. Torrelles JB, Khoo KH, Sieling PA, Modlin RL, Zhang N, Marques AM, Treumann A, Rithner CD, Brennan PJ, and Chatterjee D (2004) Truncated structural variants of lipoarabinomannan in Mycobacterium leprae and an ethambutol-resistant strain of Mycobacterium tuberculosis. J Biol Chem 279, 41227–41239 [PubMed: 15263002]
50. Guerin ME, Kaur D, Somashekar BS, Gibbs S, Gest P, Chatterjee D, Brennan PJ, and Jackson M (2009) New insights into the early steps of phosphatidylinositol mannoside biosynthesis in mycobacteria: PimB' is an essential enzyme of *Mycobacterium smegmatis*. J. Biol. Chem 284, 25687–25696 [PubMed: 19638342]
51. McCarthy RR, Mazon-Moya MJ, Moscoso JA, Hao Y, Lam JS, Bordi C, Mostowy S, and Filloux A (2017) Cyclic-di-GMP regulates lipopolysaccharide modification and contributes to

Pseudomonas aeruginosa immune evasion. Nat Microbiol 2, 17027 DOI: 10.1038/nmicrobiol.2017.27 [PubMed: 28263305]

52. Angala SK, Palcekova Z, Belardinelli JM, and Jackson M (2018) Covalent modifications of polysaccharides in mycobacteria. Nat Chem Biol 14, 193–198 [PubMed: 29443974]
53. Rose SJ, and Bermudez LE (2014) Mycobacterium avium biofilm attenuates mononuclear phagocyte function by triggering hyperstimulation and apoptosis during early infection. Infect Immun 82, 405–412 [PubMed: 24191301]
54. van Kessel JC, and Hatfull GF (2007) Recombineering in *Mycobacterium tuberculosis*. Nature Methods 4, 147–152 [PubMed: 17179933]
55. Calado Nogueira de Moura V, Gibbs S, and Jackson M (2014) Gene replacement in Mycobacterium chelonae: application to the construction of porin knock-out mutants. PloS ONE 9, e94951 DOI: 10.1371/journal.pone.0094951 [PubMed: 24739882]
56. Berg S, Starbuck J, Torrelles JB, Vissa VD, Crick DC, Chatterjee C, and Brennan PJ (2005) Roles of the conserved proline and glycosyltransferase motifs of EmbC in biosynthesis of lipoarabinomannan. J. Biol. Chem 280, 5651–5663 [PubMed: 15546869]
57. Gilleron M, Ronet C, Mempel M, Monsarrat B, Gachelin G, and Puzo G (2001) Acylation state of the phosphatidylinositol mannosides from *Mycobacterium bovis* Bacillus Calmette Guérin and ability to induce granuloma and recruit natural killer T cells. J. Biol. Chem 276, 34896–34904 [PubMed: 11441009]
58. Hawkins PT, Stephens L, and Downes CP (1986) Rapid formation of inositol 1,3,4,5-tetrakisphosphate and inositol 1,3,4-trisphosphate in rat parotid glands may both result indirectly from receptor-stimulated release of inositol 1,4,5-trisphosphate from phosphatidylinositol 4,5-bisphosphate. Biochem J 238, 507–516 [PubMed: 3026354]
59. Sartain MJ, Dick DL, Rithner CD, Crick DC, and Belisle JT (2011) Lipidomic analyses of *Mycobacterium tuberculosis* based on accurate mass measurements and the novel Mtb LipidDB. J Lipid Res 52, 861–872 [PubMed: 21285232]
60. Etienne G, Villeneuve C, Billman-Jacobe H, Astarie-Dequeker C, Dupont M-A, and Daffé M (2002) The impact of the absence of glycopeptidolipids on the ultrastructure, cell surface and cell wall properties, and phagocytosis of *Mycobacterium smegmatis*. Microbiology 148, 3089–3100 [PubMed: 12368442]
61. Rose SJ, and Bermudez LE (2016) Identification of Bicarbonate as a Trigger and Genes Involved with Extracellular DNA Export in Mycobacterial Biofilms. mBio 7 DOI: 10.1128/mBio.01597-16
62. Martin A, Camacho M, Portaels F, and Palomino J-C (2003) Resazurin microtiter assay plate testing of *Mycobacterium tuberculosis* susceptibilities to second-line drugs: rapid, simple, and inexpensive method. Antimicrob. Agents Chemother 47, 3616–3619 [PubMed: 14576129]

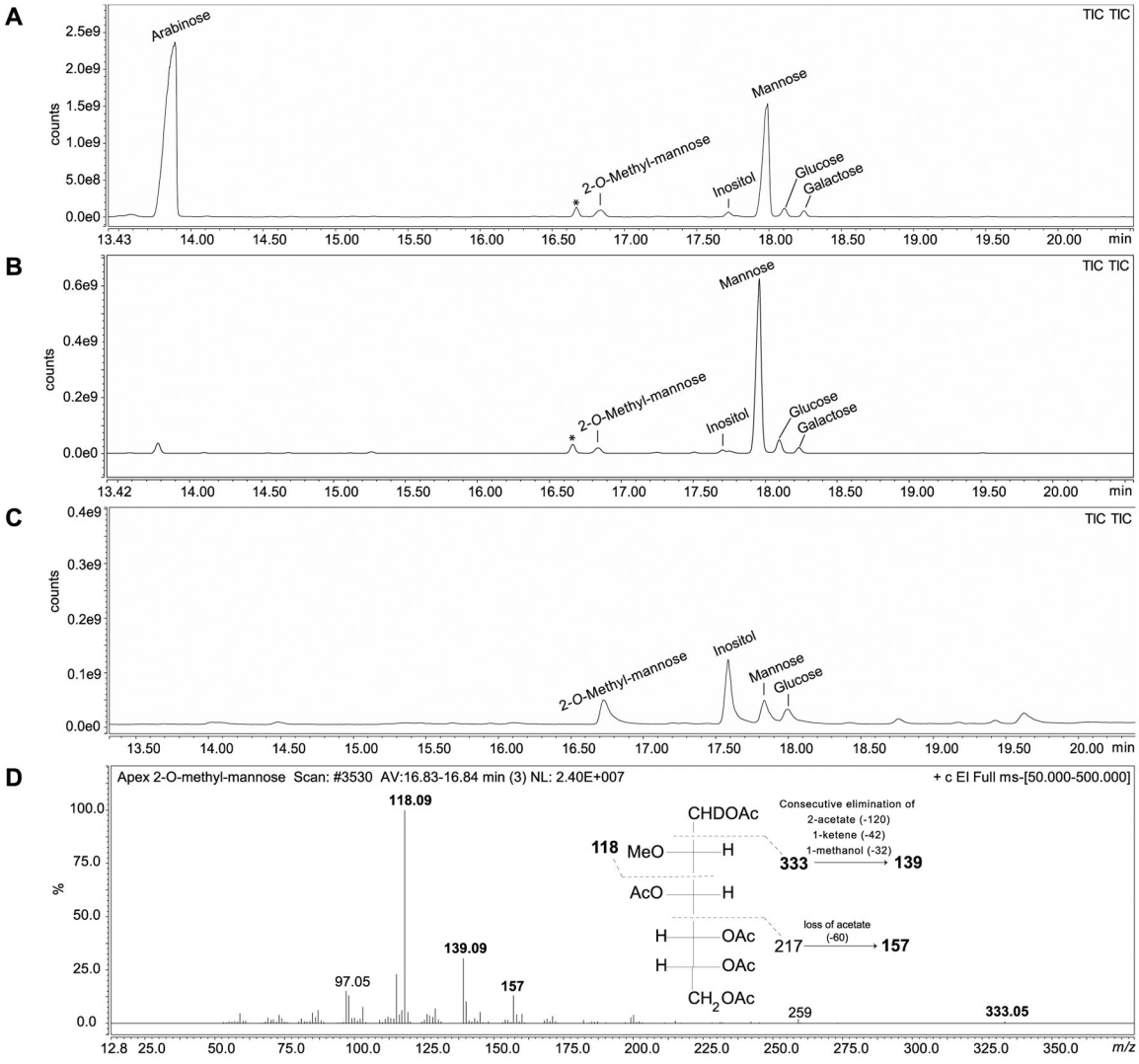

Figure 1: Monosaccharidic composition of LAM, LM and phosphatidylinositol dimannosides from WT *Mabs* ATCC 19977.

GC/MS analysis of alditol acetate derivatives prepared from WT *Mabs* LAM (A), LM (B) and PIM_2 (C). (D) Extracted ion mass spectrum and structure corresponding to the peak identified as 2-*O*-methylmannose with retention time 16.83 min and characteristic ions with *m/z* 118, 139, 157 and 333. This peak was detected in all three samples. *Non-carbohydrate contaminant.

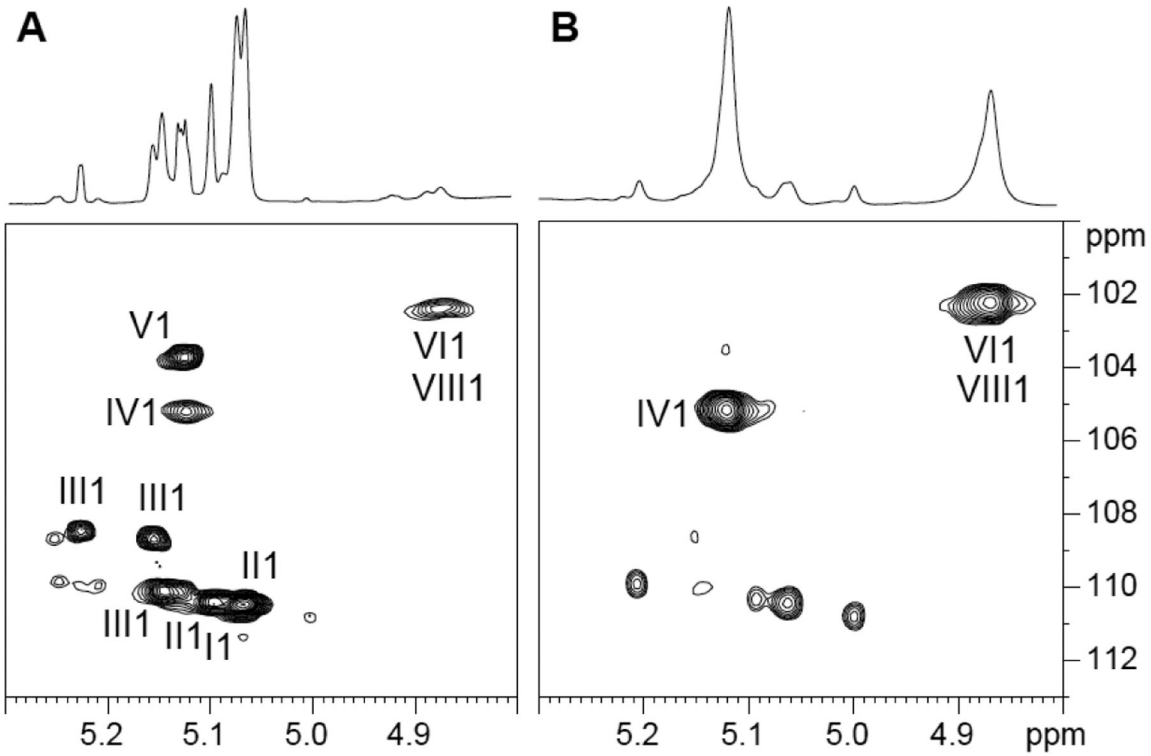

Figure 2: Branching of the mannan domain of LM and LAM from Mabs ATCC 19977.
Expanded region (δ ^{1}H: 4.80–5.30, δ ^{13}C 100–113) of the 2D ^{1}H-^{13}C HMQC spectrum in D_2O at 298K of LAM (A) and LM (B) from WT *Mabs* ATCC 19977. I, 3,5 α-Ara*f*; II, 5 α-Ara*f*; III, 2 α-Ara*f*; IV, t-α Man*p*; V, β-Ara*f*; VI, 6 α Man*p*; VIII, 3,6 α Man*p*.

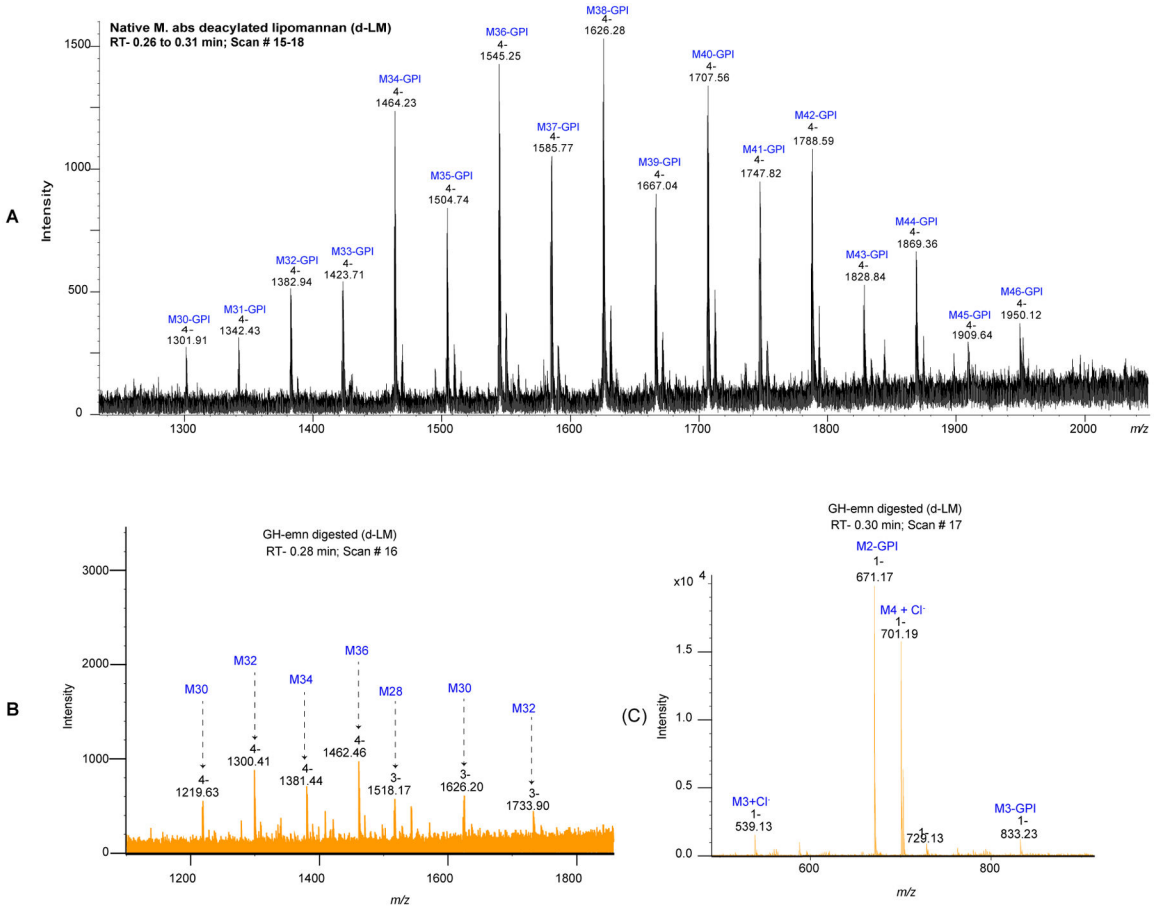

Figure 3: Negative ion liquid chromatography-mass spectrometry (LC-MS) analysis of the Mabs deacylated LM (d-LM) before and after digestion with α−1,6-endomannanase (GH-emn).

(A) LC-MS profile of *Mabs* d-LM before enzymatic treatment. The mass spectrum is dominated by a series of quadruply-charged ions corresponding to the high molecular weight mannan backbone containing 30 to 46 mannosyl residues [M30 to M46] (range of 5,000 to 7,800 Da). (B-C) LC-MS profile of *Mabs* d-LM after treatment with the GH-emn α−1,6-endomannanase. The mass spectrum at 0.28 min retention time (B) corresponds to oligomannans (lacking the glycerol-phosphatidyl inositol anchor [GPI]) with an even number of mannosyl residues from M28 to M36. The mass spectrum at 0.30 min retention time (C) shows two major ions corresponding to the mass of methylated species of d-PIM2 (*m/z* 671.17 [M-H]), and a tetra-mannoside (M4) lacking the GPI anchor (*m/z* 701.19 [M +Cl]$^{-}$).

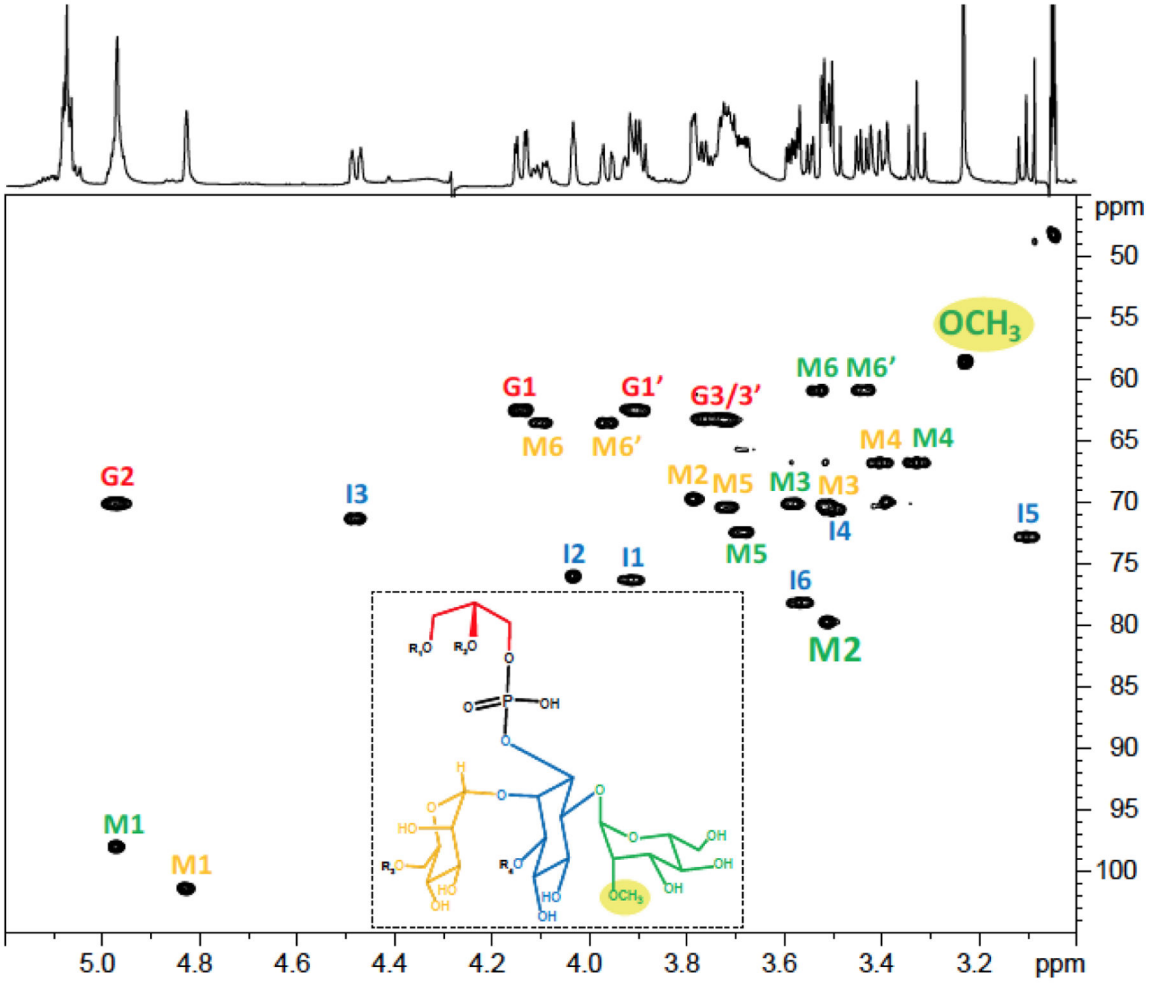

Figure 4: Presence of a methyl group on Mabs ATCC 19977 tetra-acylated PIM2.

^{1}H-^{13}C HMQC spectrum of the tetra-acylated PIM_2 from WT *Mabs* ATCC 19977 in $CDCl_3/CD_3OD/D_2O$, 60:35:8 (v/v/v) at 298 K. The mannose unit (M) in green is the one located on position 6 of *myo*-Ins (I); the mannose unit in yellow is the one located on position 2 of *myo*-Ins; the Gro unit is symbolized (G). R1–4 correspond to fatty acyl chains.

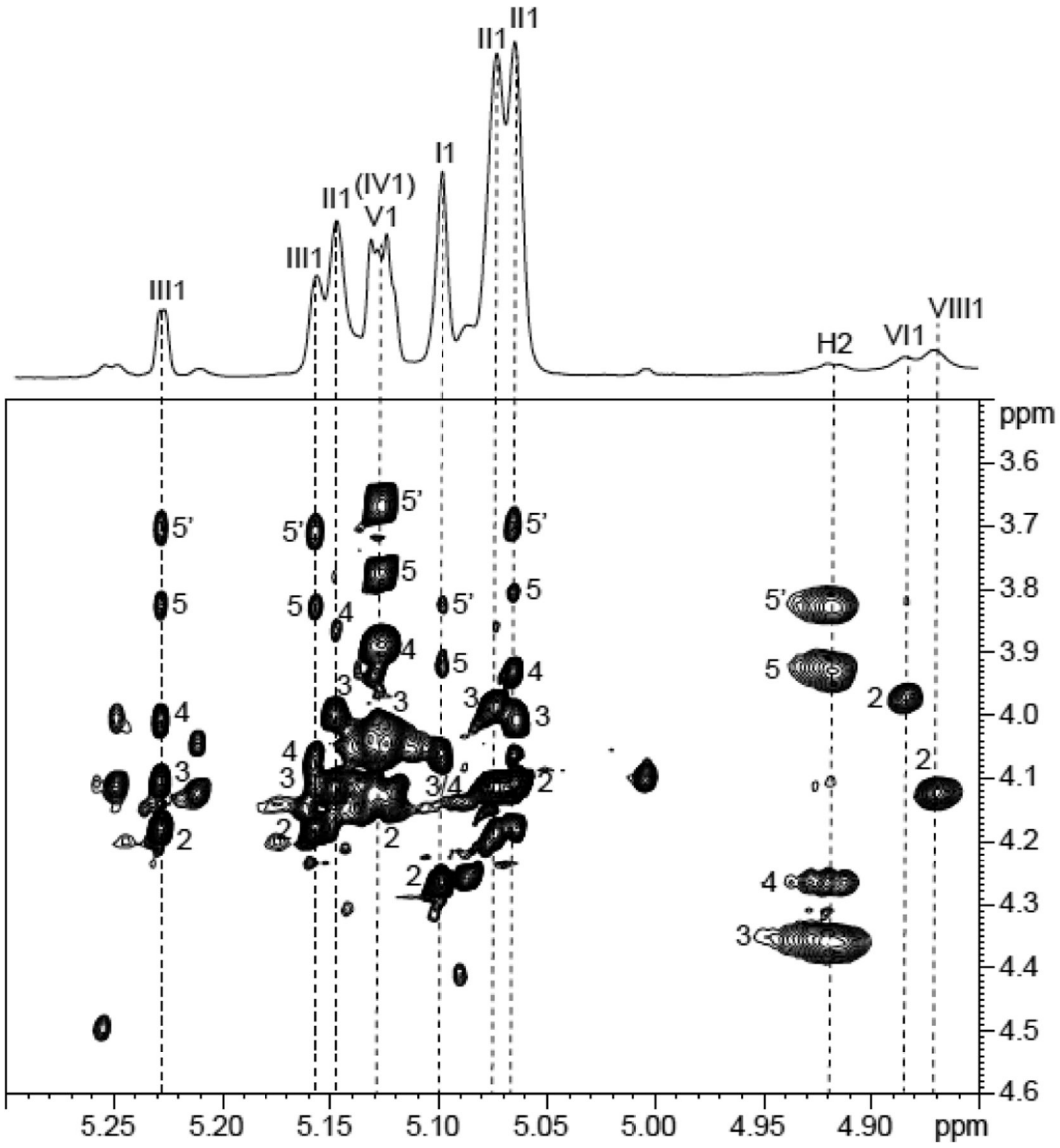

Figure 5: Characterization of the different units of Mabs ATCC 19977 LAM by NMR.

Expanded region (δ F2 5.30–4.85 and δ F1 3.5–4.6) of the ^{1}H-^{1}H TOCSY spectrum of LAM from WT *Mabs* ATCC 19977 dissolved in D_2O at 298 K. I, 3,5 α-Ara*f*; II, 5 α-Ara*f*; III, 2 α-Ara*f*; IV, t-α Man*p*; V, β-Ara*f*; VI, 6 α Man*p*; VIII, 3,6 α Man*p*. Numerals correspond to proton number. H2 corresponds to the H-2 of the arabinosyl units bearing the succinyl residues.

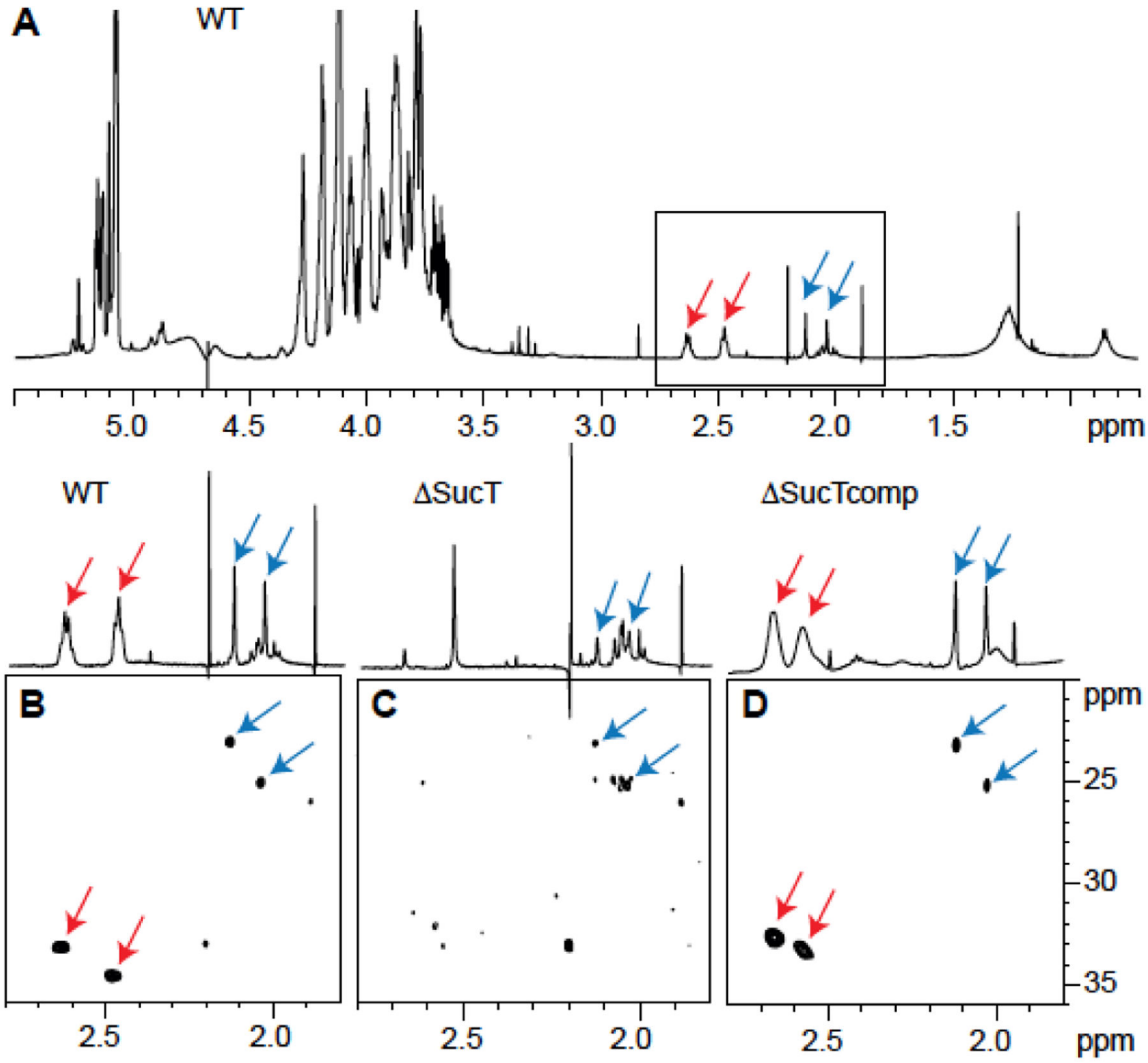

Figure 6: Presence of acetate and succinate residues on WT Mabs LAM.

NMR analysis of LAM prepared from the WT, mutant (Δ*sucT*), and complemented mutant (Δ*sucT*comp) strains. Shown are 1D ^{1}H (A) and expanded region (δ ^{1}H 2.80–1.80 and δ ^{13}C 36–20) of the 2D ^{1}H-^{13}C (B-D) HMQC NMR spectra. Arrows point to the signals typifying acetates (blue) and succinates (red) (see text for details).

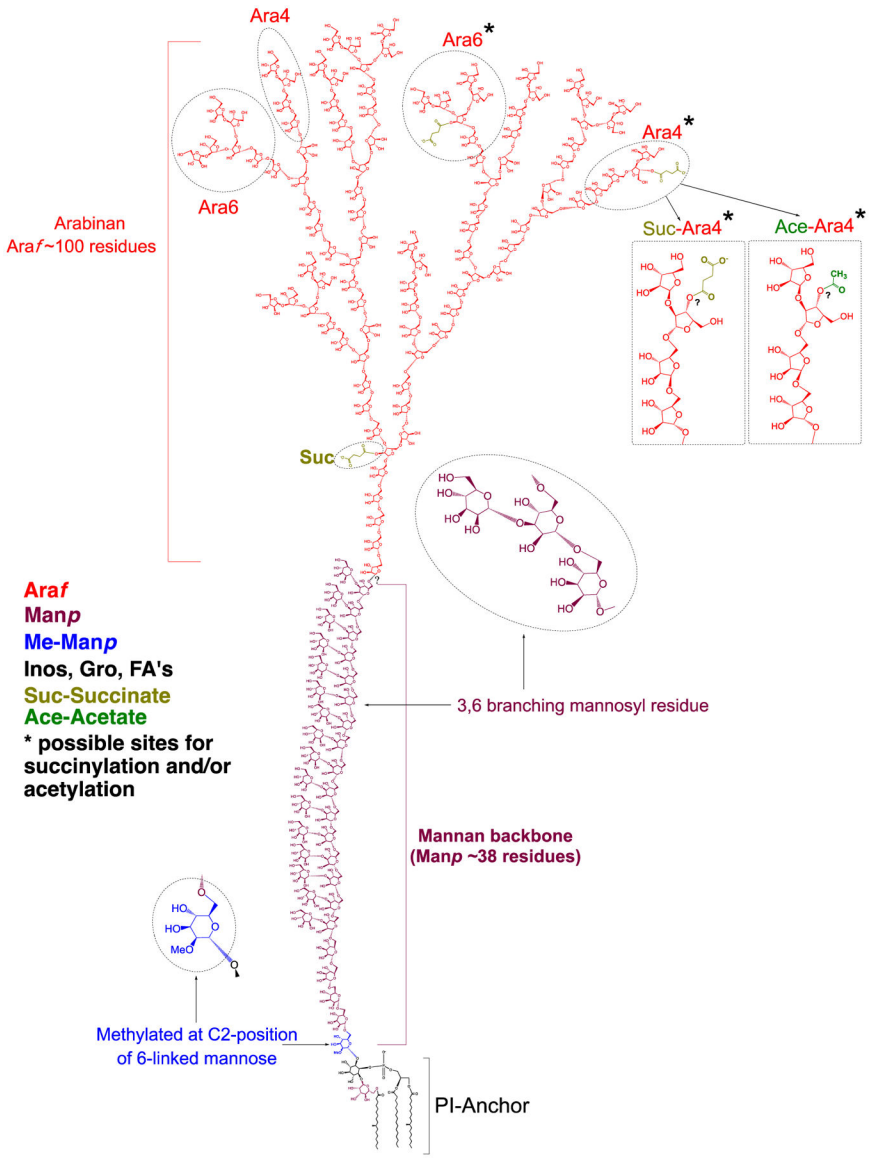

Figure 7: Proposed structure of Mabs LAM, consistent with available data.

The non-reducing arabinan termini of *Mabs* LAM are devoid of capping residues. The core structure of the arabinan domain consists of ~ 100 D-Ara*f* residues including linear α−1,5-linked residues and α−1,3 branch points. The arabinan domain is terminated with β-D-Ara*f*-1,2-α-D-Ara*f* at the non-reducing end and there is an equal proportion of linear Ara_4 and branched Ara_6 arabinan termini. Succinyl residues substitute both internal and terminal arabinosyl residues whereas acetyl residues substitute terminal arabinosyl residues. The precise positions of the succinyl and acetyl residues substituting the terminal arabinosyl residues are currently not known. The mannan backbone with 38 α-D-Man*p* residues (dominant species per Figure 3A) is composed of linear α−1,6-linked residues and α−3,6 branch points. A single α−1,6-linked Man*p* residue located at the reducing end of the mannan backbone is methylated at the C-2 position. Further analyses are required to determine the covalent linkage of the arabinan domain to the mannan backbone and the

precise structural organization of these two domains. Inos, Inositol; Gro, glycerol; FA, fatty acyl chains.

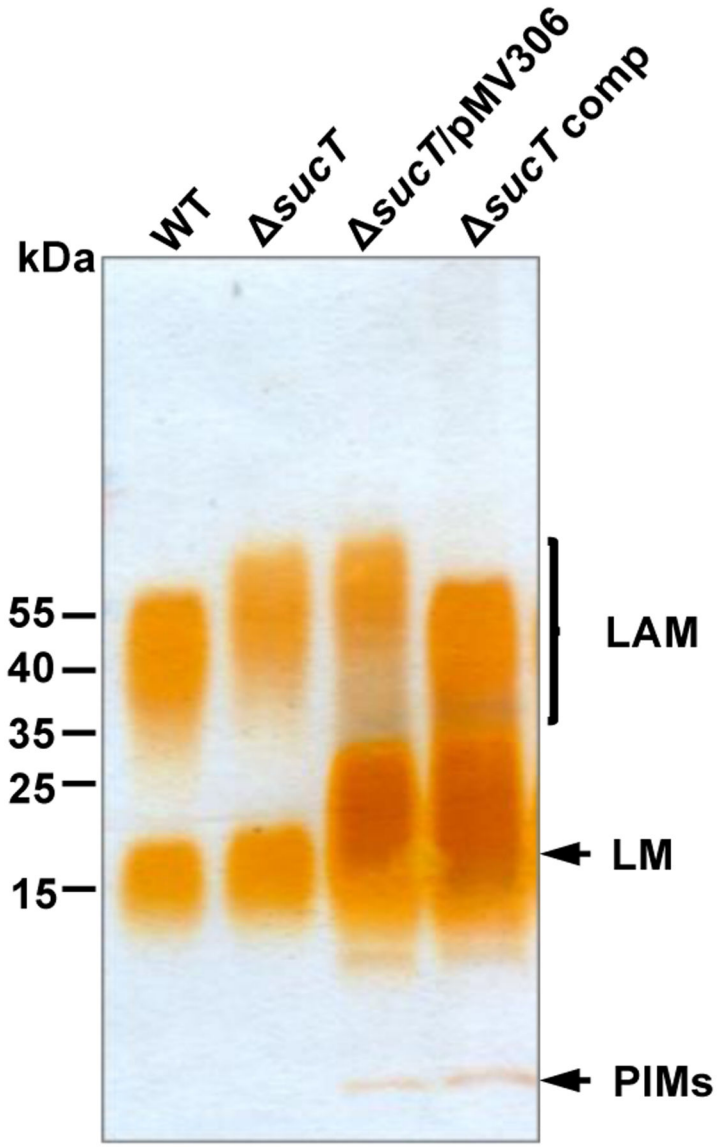

Figure 8: Electrophoretic mobility of lipoglycans from WT Mabs ATCC 19977, the sucT mutant and the complemented sucT mutant.

Lipoglycans extracted from WT *Mabs* ATCC 19977, *Mabs*Δ*sucT*, *Mabs*Δ*sucT* harboring an empty pMV306 plasmid, and *Mabs*Δ*sucT*/pMV306-*sucT* (Δ*sucT* comp) were run on a 10–20% Tricine gel followed by periodic acid-silver staining. The results presented are representative of three independent SDS-PAGE runs using different lipoglycan preparations from each strain.

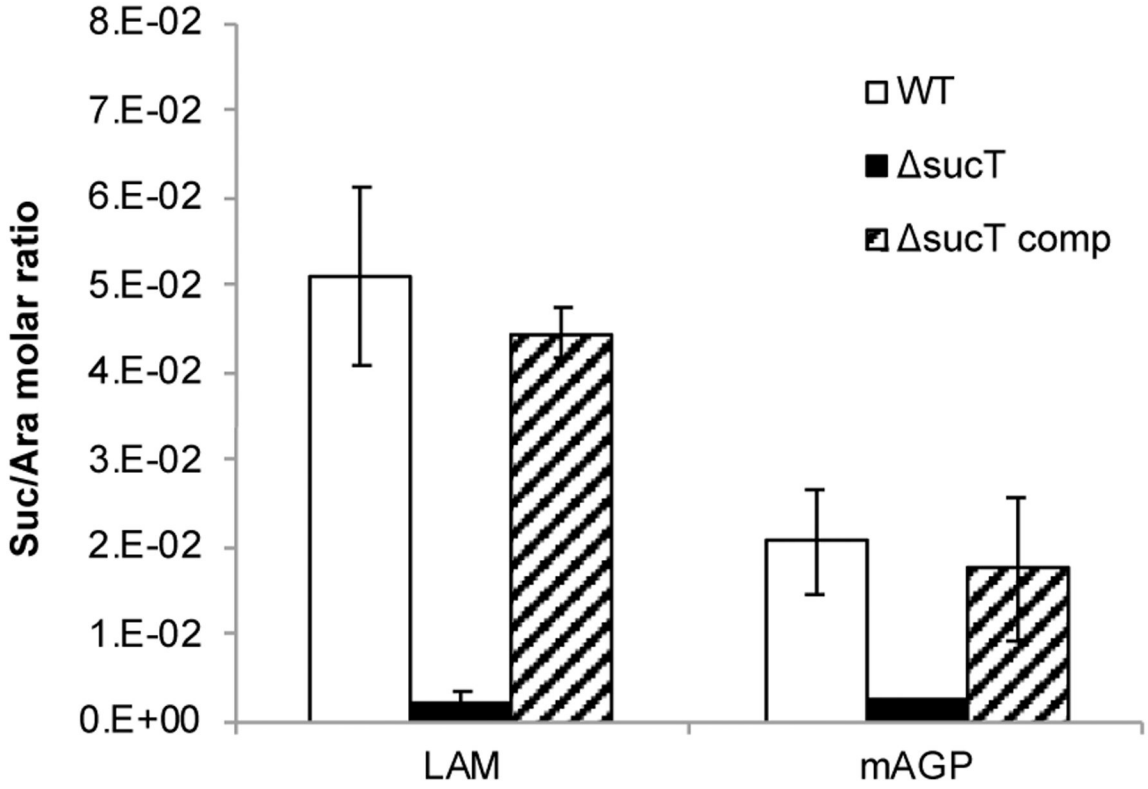

Figure 9: Succinate content of AG and LAM prepared from WT Mabs ATCC 19977, the sucT mutant and the complemented mutant strain.

Quantification of succinates and arabinose residues in the same LAM and mAGP samples prepared from the WT, mutant and complemented mutant strains. Results are expressed as average ± SD succinate/arabinose molar ratios from three technical replicates.

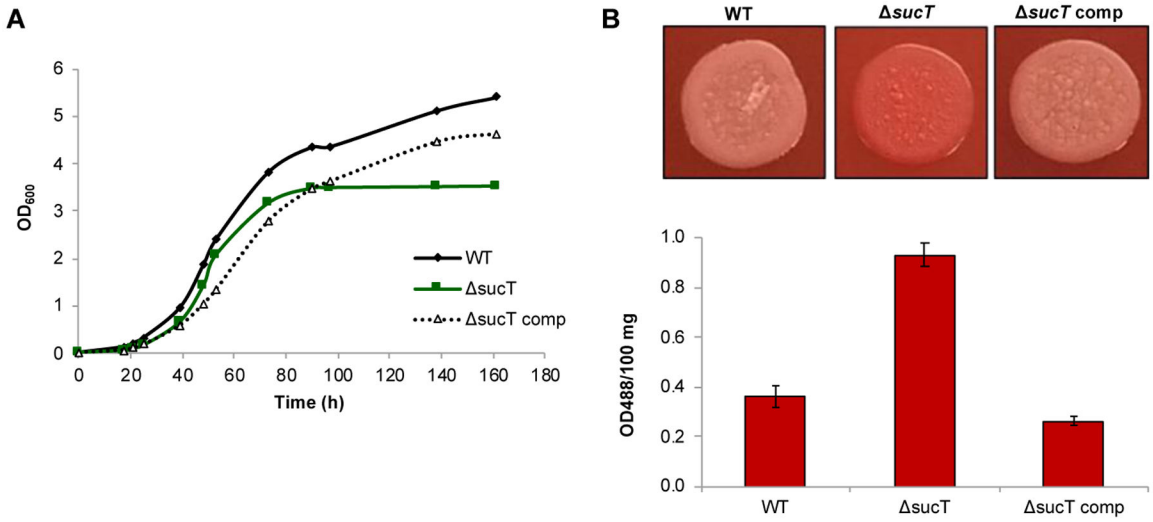

Figure 10: Growth characteristics and cell envelope properties of the Mabs sucT mutant.

(A) Growth characteristics of WT *Mabs* ATCC 19977, the *sucT* mutant and the complemented mutant strain in 7H9-ADC-Tween 80 at 37°C. The results presented are representative of three independent experiments.

(B) Congo red binding on TS agar plate (top panel) and in TS liquid medium (graph). Shown on the graph are the average ± SD absorbances of acetone extracts measured for three biological replicates.

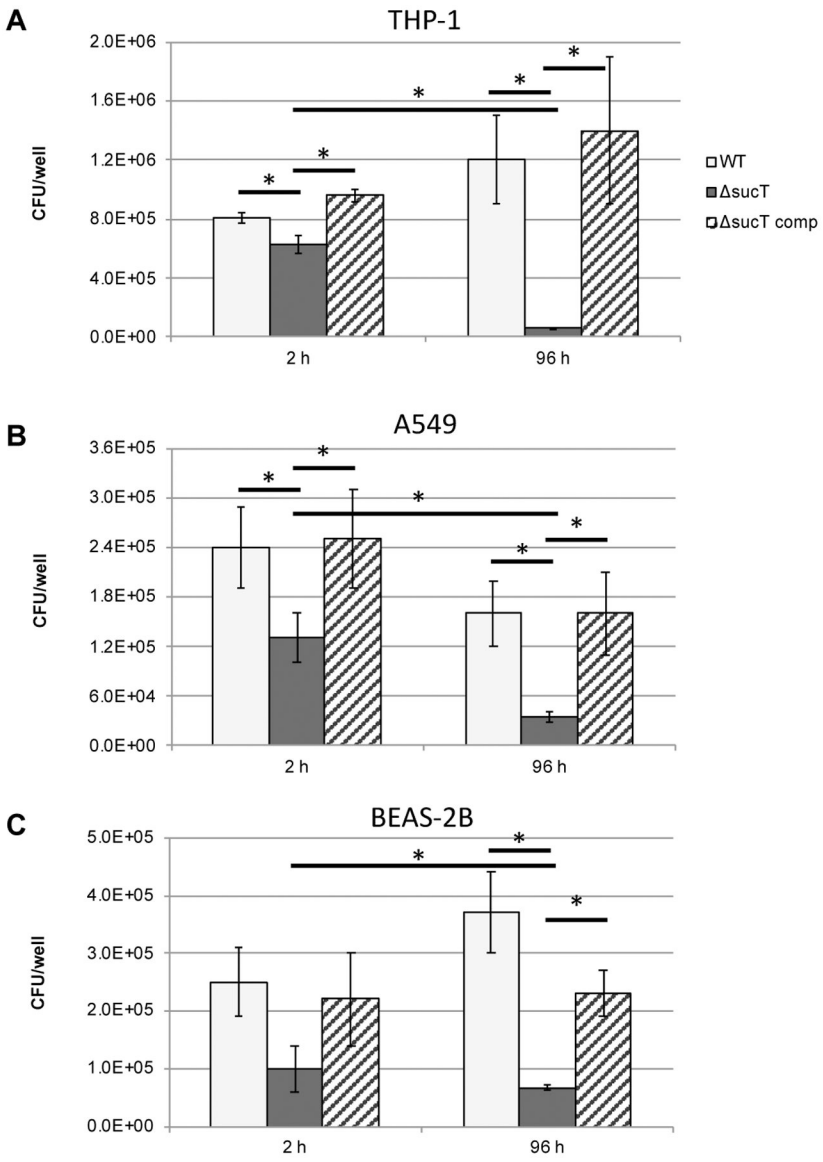

Figure 11: Invasion and intracellular replication of Mabs WT, mutant and complemented mutant strains in (A) THP-1 macrophages, (B) A549 lung alveolar type II epithelial cells and (C) BEAS-2B bronchial mucosal epithelial cells.

Cells were infected at a MOI of 10 bacteria per cell and intracellular CFUs counted after 2 and 96 hours of infection. Data is shown as mean values + SD of triplicate wells. Statistical analysis using 2-way ANOVA, *$p<0.05$. The results presented are representative of three independent experiments.

Table 1:

^{1}H and ^{13}C NMR chemical shifts of LM from WT *Mabs* ATCC 19977 measured at 298K in D_2O.

		1	2	3	4	5	6
t*Man*p	**^{13}C**	105.1	72.99	73.65	69.70	76.20	63.90
	^{1}H	5.12	4.06	3.86	3.65	3.76	3.76/3.87
6Man*p*	**^{13}C**	102.15	72.44	73.65	69.70	nd	69.65
	^{1}H	4.87	3.97	3.86	3.65	nd	3.76 / 3.88
3,6Man*p*	**^{13}C**	102.15	72.86	81.29	68.79	73.34	68.24
	^{1}H	4.87	4.12	3.91	3.86	3.87	3.75/3.94

Table 2:

^{1}H and ^{13}C NMR chemical shifts of tetra-acylated PIM_2 from WT *Mabs* ATCC 19977 measured at 298K in $CDCl_3/CD_3OD/D_2O$, 60:35:8, v/v/v.

		1	2	3	4	5	6
Man1 on 6Ins	**^{13}C**	98.01	79.78	70.12	66.79	72.46	60.90
	^{1}H	4.97	3.51	3.59	3.33	3.69	3.44/3.54
Man2 on 2Ins	**^{13}C**	101.44	69.73	70.34	66.77	70.42	63.55
	^{1}H	4.83	3.79	3.51	3.41	3.72	3.97 / 4.10
***myo*-Ins**	**^{13}C**	76.33	76.04	71.36	70.61	72.84	78.18
	^{1}H	3.92	4.04	4.48	3.49	3.10	3.57
Gro	**^{13}C**	62.51	70.12	63.29			
	^{1}H	3.91 / 4.14	4.97	3.76 / 3.72			